The FASEB Journal express article 10.1096/fj.03-0501fje. Published online November 20, 2003.

Glucocorticoid receptor deficiency increases vulnerability of the nigrostriatal dopaminergic system: critical role of glial nitric oxide

Maria Concetta Morale,* Pier Andrea Serra,[†] Maria Rosaria Delogu,[†] Rossana Migheli,[†] Gaia Rocchitta,[†] Cataldo Tirolo,* Salvo Caniglia,* Nuccio Testa,* Francesca L'Episcopo,* Florinda Gennuso,* Giovanna M. Scoto,[‡] Nicholas Barden,[§] Egidio Miele,[†] Maria Speranza Desole,[†] and Bianca Marchetti,*[,†]

*OASI Institute for Research and Care on Mental Retardation and Brain Aging (IRCCS), Neuropharmacology Section, Troina, Italy; [†]Department of Pharmacology, Faculty of Medicine, University of Sassari, Italy, [‡]Department of Pharmacology, Faculty of Pharmacy, University of Catania, Italy; and the [§]CHUL Research Centre and Department of Anatomy and Physiology, Laval University, Quebec, Canada

Corresponding author: Bianca Marchetti, Neuropharmacology, OASI Institute for Research and Care on Mental Retardation and Brain Aging (IRCCS), Via Conte Ruggero 73, 94018 Troina (EN) Italy. E-mail: bianca.marchetti@oasi.en.it

ASTRACT

Glucocorticoids (GCs) exert via glucocorticoid receptors (GRs) potent anti-inflammatory and immunosuppressive effects. Emerging evidence indicates that an inflammatory process is involved in dopaminergic nigro-striatal neuronal loss in Parkinson's disease. We here report that the GR deficiency of transgenic (Tg) mice expressing GR antisense RNA from early embryonic life has a dramatic impact in "programming" the vulnerability of dopaminergic neurons to 1-methyl-4-phenyl-1,2,3,6-tetrahydropyridine (MPTP). The GR deficiency of Tg mice exacerbates MPTP-induced toxicity to dopaminergic neurons, as revealed by both severe loss of tyrosine hydroxylase positive nigral neurons and sharp decreases in striatal levels of dopamine and its metabolites. In addition, the late increase in dopamine oxidative metabolism and ascorbic acid oxidative status in GR-deficient mice was far greater than in wild-type (Wt) mice. Inducible nitric oxide synthase (iNOS) was sharply increased in activated astrocytes, macrophages/microglia of GR-deficient as compared with Wt mice. Moreover, GR-deficient microglia produced three- to fourfold higher nitrite levels than Wt mice; these increases preceded the loss of dopaminergic function and were resistant to GR the inhibitory effect of GC, pointing to peroxynitrites as candidate neurotoxic effectors. The iNOS inhibitor N^6-(1-iminoethyl)-L-lysine normalized vulnerability of Tg mice, thus establishing a novel link between genetic impairment of GR function and vulnerability to MPTP.

Key words: Parkinson's disease (PD) • inflammation • hypothalamic-pituitary-adrenocortical (HPA) axis • astroglial inducible nitric oxide synthase (iNOS) • neuroprotection

Downloaded from www.fasebj.org to IP 151.97.98.252. *The FASEB Journal* Vol., No. , pp:, November, 2016

Glucocorticoid hormones (GCs)[1] regulate various physiological responses and developmental processes by binding to and modulating the transcriptional activity of their cognate receptors. GCs are predominantly released upon stress to maintain homeostasis and play important roles in a variety of brain functions, including cognition, emotion, and feeding (1–3). Under physiological conditions, GCs are adaptive and beneficial; however, prolonged elevation of GCs levels is believed to contribute to neurodegeneration and brain dysfunction (2–4). Different aspects of the effects of GCs have been addressed, including anatomical diversity of the brain region involved, species and strain differences, involvement of excitotoxins, metabolic pathways or neurotrophin factor synthesis, but the interaction of GCs with the immune system has received less attention. Indeed, GCs exert potent anti-inflammatory and immunosuppressive effects and are key regulators of the bi-directional communication between the neuroendocrine and immune systems (5–8). As a consequence of this interaction, the secretion of GC from the adrenal glands increases during an immune response, and this mechanism limits the magnitude of the inflammatory reaction to an immunogenic stimulus.

GCs exert their immune regulatory effects at multiple levels after binding to their cytoplasmatic receptors (Type II, or GRs), which are primarily involved in the feedback regulation of the hypothalamic-pituitary-adrenocortical (HPA) axis (1, 2). Upon ligand binding, GR translocates into the nucleus and regulates gene expression, resulting in down-regulation of a wide variety of pro-inflammatory cytokines and immune mediators (9), including nitric oxide (NO), a key molecule in the inflammatory response (10). An important molecular mechanism recognized to underlie most of the anti-inflammatory and immunosuppressive activity GCs is inhibition of the activation of protein-1 (AP-1, Jun-Fos heterodimers) and nuclear factor kB (NF-kB, p65-p50 heterodimers) families of transcription factors (11–13). In particular, the cytokine-dependent stimulation of inducible nitric oxide synthase (iNOS or NOS2), responsible for NO production, is mediated by NF-kB activation and is efficiently suppressed by GCs (14, 15).

Increasing experimental, clinical, and epidemiologic studies point to a pivotal role of inflammation and oxidative stress in the pathogenesis of acute or chronic neurodegenerative diseases (16–18). Particularly, in the context of innate inflammatory mechanisms, glia appears to play important roles in a wide range of neurodegenerative disorders, including Parkinson's disease (PD; 19–21). Selective degeneration of dopaminergic neurons in the substantia nigra pars compacta (SN) and focal gliosis are pathological hallmarks of PD and of 1-methyl-4-phenyl-1,2,3,6-tetrahydropyridine (MPTP)-induced experimental PD in many species, including humans, monkeys, and mice (22–24). After systemic administration, MPTP readily enters the brain and is metabolized by astroglia to 1 methyl-4-phenylpyridinium (MPP^+; 25). MPP^+ is a substrate of the dopamine transporter, and it is concentrated in nigral dopaminergic neurons where it inhibits Complex I of the mitocondrial electron transport chain, resulting in ATP depletion and subsequent neuronal death (25). Recent evidence, however, indicates that glial dysfunction may contribute to PD pathology through the release of toxic substances, causing dopaminergic cell death and/or increasing neuronal vulnerability to neurotoxins (26–30). In particular, microglial-derived iNOS/NO, alone or in cooperation with superoxide anion and peroxynitrites, are emerging as predominant effectors of MPTP-induced neuronal death (26–34). Recently, association between PD and polymorphism of neuronal NO synthase (nNOS) and iNOS genes have been described (35). Of special interest, reactive astrocytes, which synthesize various neurotrophic factors upon brain injury and actively participate in repair processes (36–

Downloaded from www.fasebj.org to IP 151.97.98.252. *The FASEB Journal* Vol., No. , pp:, November, 2016

38), have been suggested to play a key role in the sequential linkage of neurochemical and cellular events leading to MPTP-induced nigral dopaminergic neuron death (39).

Several neurological diseases are accompanied by dysregulation of the HPA axis. Transgenic (Tg) mice expressing from early embryonic life anti-sense RNA directed against GRs were created to serve as animal models for the study of neuroendocrine changes occurring in stress-related disorders (40). These mice show reduced GRs mRNA in the brain, pituitary, and immune organs; reduced GRs binding; and reduced HPA axis sensitivity to GCs (40–44). As a consequence of dysfunction of GRs, these Tg mice exhibit an aberrant response to stressful and immunogenic stimuli (45–49). We recently reported that the GR-deficiency renders these Tg mice resistant to myelin oligodendrocyte glycoprotein (MOG)-induced autoimmune encephalomyelitis (EAE), via NO-induced immunosuppression (50). There is a growing appreciation that the pre-perinatal exposure to abnormal GC levels may alter the developmental programming of the HPA axis and stress response, as well as modulate the susceptibility to inflammatory and autoimmune diseases (6, 7, 50–54). Here we investigated the impact of lifelong GR deficiency of these Tg mice in the vulnerability of the nigrostriatal dopaminergic system to MPTP.

MATERIALS AND METHODS

Animals

Female B6C3F1 (C57B female × C3H male) [H-2^b] wild-type (Wt) and Tg (line 1.3) mice, in which a transgene driven by a neurofilament promotor was inserted in the genome constitutively expressing antisense RNA against the GRs (40), were bred at the OASI Institute, (Troina, EN, Italy). The mRNA levels and binding capacity of GRs in the brain, pituitary, and immune organs of these Tg mice are decreased by ~40–50% compared with Wt mice (40, 43). Mice of 2–3 months of age (body weight 20–25 g) were housed five per cage in a temperature (21–23°C), humidity (60%), and light (50/50 light:dark cycle, lights on at 06:00 a.m.) controlled room. Food and tap water were available ad libitum. Studies were conducted in accordance with the Guide for the Care and Use of Laboratory Animals (NIH) and were approved by the Review Boards of the OASI Institute (Troina, Italy).

MPTP administration

MPTP-HCl (Research Biochemical International, Natick, MA) 30 mg/kg was given intraperitoneally, at 24 h intervals, for five consecutive days (39), to groups of Wt and GR-deficient mice. This dosage is below that producing necrotic cell death (39). Wt and GR-deficient mice injected with vehicle (saline, 2 ml/kg intraperitoneally) served as control. Wt and GR-deficient control and MPTP-treated mice were killed at different days (1, 7, 11, or 21) after MPTP discontinuance by quick decapitation, between 08:00 and 12:00 a.m. Great care was taken to keep the mice undisturbed the night before the experiment. Trunk blood was collected after decapitation, and the plasma was stored at –80°C for corticosterone assay by using a specific RIA (ICN Biomedical, Costa Mesa, CA), as reported (40, 43). Heads were cooled by rapid immersion in liquid nitrogen. Thereafter, striata of both sides were rapidly removed and frozen at –80°C for subsequent HPLC determination of neurochemicals as described previously (39).

Downloaded from www.fasebj.org to IP 151.97.98.252. *The FASEB Journal* Vol., No. , pp:, November, 2016

HPLC determination of striatal neurochemicals

Dopamine, dihydroxyphenylacetic acid (DOPAC), homovanillic acid (HVA), 3-methoxytyramine (3-MT), 5-hydroxytryptamine (5-HT), 5-hydroxyindoleacetic acid (5-HIAA), ascorbic acid, and dehydroascorbic acid (DHAA) were performed by HPLC according to methods described previously (39). Striata of both sides, removed 1, 7, and 11 days after MPTP discontinuance, were pooled, weighed, and homogenized in 1% meta-H_3PO_4 containing EDTA 1 mM. After centrifugation (17,500 g for 10 min at 4°C), the supernatant was divided into two aliquots. The first was filtered and immediately injected into the HPLC system for dopamine, DOPAC, HVA, 3-MT, and ascorbic acid and uric acid determinations. HPLC with electrochemical detection was performed with a high-pressure pump Varian 9001 with a Rheodyne injector, column 15 cm × 4.6 mm i.d. TSK-ODS-80 TM, electrochemical detector BAS LC-4B, and integrator Spectra-Physics SP 4290 (39). The mobile phase was citric acid 0.1 M, K_2HPO_4 0.1 M, EDTA 1 mM, MeOH 5%, and sodium octylsulphate 70 mg/l (pH=3.0); the flow rate was 1.2 ml/min and 10 μl of sample were injected. The second aliquot was adjusted to pH 7.0 with K_2HPO_4 45% and DL-homocysteine 1% was added to reduce DHAA to ascorbic acid. The sample was incubated for 30 min at 25°C, then adjusted to pH 3.0 with metaH_3PO_4 30%, filtered and injected (20 μl) for total ascorbic acid determination. DHAA concentration was calculated from the difference in ascorbic acid content between the first and second aliquot (39).

High-affinity [^{3}H]dopamine uptake assay

To investigate the ability of Wt and GR-deficient mice to recover from MPTP neurotoxic effects, mice (five animals/group) were given a single MPTP injection (55 mg/kg intraperitoneally), according to Ho and Blum (38). Mice were killed 1, 7, 11, and 21 days after MPTP injection. Left and right striata were homogenized in ice-cold pre-lysis buffer (10 mM Tris, pH 7.5, and 0.32 M sucrose) by using a Teflon pestle-glass mortar and homogenized tissue centrifuged for 10 min at 1000 × g at 4°C to remove nuclei. The supernatant containing the synaptosomes was collected, aliquots were removed for the determination of protein concentration and dopamine uptake (total high affinity and mazindol noninhibitable). Supernatant (50 μl) was diluted in Krebs-Ringer phosphate buffer (16 mM NaH_2PO_4, 16 mM Na_2HPO_4, 119 mM NaCl, 4.7 mM KCl, 1.8 mM $CaCl_2$, 1.2 mM $MgSO_4$, 1.3 mM EDTA, and 5.6 mM glucose; pH 7.4) and incubated at 37°C in the presence or absence of mazindol (10 μM), a high-affinity dopamine up-take inhibitor. [^{3}H]Dopamine (25 nM, specific activity, 20–40 Ci/mmol; Amersham, Arlington Heights, IL) was added in Krebs-Ringer buffer and incubation was carried on for 6 min at 37°C. Synaptosomes were collected on presoaked nitrocellulose filters by filtration and non-specific radioactivity was washed with Krebs-Ringer phosphate buffer followed by filtration. The filters were then transferred into scintillation vials and measured by liquid scintillation (Cytoshint; ICN, Costa Mesa, CA) counter (Packard). Specific high-affinity neuronal dopamine up-take is expressed as fentomoles of dopamine uptake per microgram of protein minus the fentomoles of mazindol uptake. Values are represented by the changes in dopamine uptake (expressed as percent of control). Proteins were measured by the method of Lowry et al. (55).

Downloaded from www.fasebj.org to IP 151.97.98.252. *The FASEB Journal* Vol., No. , pp:, November, 2016

Immunocytochemistry

On the day the mice were killed (six mice/experimental group), they were anesthetized by intraperitoneal injection of Nembutal (50 mg/kg). Mice were rapidly perfused transcardially with 0.9% saline, followed by 4% paraformaldehyde in phosphate buffer (pH 7.2 at 4°C). Brains were carefully removed and post-fixed for 2–4 h, in 4% paraformaldehyde in phosphate buffer (pH 7.2) and placed in 15% sucrose in the solution of phosphate buffer overnight at 4°C. Tissues were frozen at –80°C. Serial cryostat sections (10 μm, from the olfactory bulb to the end of the medulla), were collected, mounted on poly-L-lysine-coated slides and processed for immunocytochemistry (56–58). Identification of the level was made by comparison with the sections of the mouse brain (59). All immunostaining procedures were performed on sections incubated in blocking buffer (0.3–0.5% Triton X-100, 5% BSA, and 5% serum in PBS) for 30 min followed by an overnight incubation with the following primary antibodies in blocking buffer at 4°C: (i) tyrosine hydroxylase (TH; goat polyclonal, anti-TH, Santa Cruz Biotechnology, Santa Cruz, CA) as a marker of dopaminergic neurons 1:200; (ii) glial fibrillary acidic protein (goat polyclonal, anti-GFAP, Santa Cruz Biotechnology) 1:100; (iii) rabbit anti-GFAP, DAKO, DK-2600 Glostrup, Denmark) for astrocytes 1:200; (iv) membranolytic attack complex of complement (rat monoclonal, anti-mouse Mac-1/CD11b, PharMingen International, Becton Dickinson, San Jose, CA) for activated macrophages/microglia 1:100; (v) inducible nitric oxide synthase (rabbit polyclonal, anti-iNOS, Santa Cruz Biotechnology) 1:100; and (vi) nitrotyrosine (rabbit anti-NT, Upstate, Lake Placid, NY) 1:200, to reveal nitrosative reactions. All antibodies, whether used for single or dual labeling procedures, were visualized by immunofluorescence (56–58), TH-Ab was also visualized by using immunoperoxidase (for single labeling stereological quantitation). Sections were incubated overnight at 4°C with the indicated dilutions of the antibodies, either alone or in combination as described. After three (× 5 min) washes in PBS, primary antibodies were revealed with specific FITC and CY3 conjugated secondary antibodies 1:100–1:200 dilution. (60 min at room temp). After three (× 5 min) washes in PBS, cells were mounted with Gel mounting solution (Biomeda Corp. Foster City, CA). In all of these protocols, blanks were processed as for experimental samples except that the primary antibodies were replaced with PBS. For quantification of TH-IR neurons, striatal and mid-brain 10 μm coronal sections [bregma 1.34 mm to bregma –0.82 mm for striatum; bregma –2.46 mm to bregma –3.88 mm for SN according to Franklin and Paxinos (59)], were counterstained with the nuclear counterstain Methyl Green (Vector Laboratories Inc. Burlingame, CA). All sections (from Wt and Tg mice) were stained simultaneously by using the same solutions and conditions. The total number of TH-IR cell bodies was estimated and examined in a blind fashion (60).

Confocal laser microscopy and image analysis

Sections labeled by immunofluorescence were visualized and analyzed with a confocal laser scanning microscope LEICA TCS NT (Version 1.0, Leica Lasertechnik GmBH, Heidelberg, Germany), equipped with an argon/krypton laser using 10, 20, and 40, and 100 × oil-immersion objectives (56–58). Pinhole was set at 1–1.3 for optical sections of 0.48–0.5 μm. Single lower power scans were followed by 16 to 22 serial optical sections of 4–6 fields per section. Laser attenuation, pinhole diameter, photomultiplier sensitivity, and off-set were kept constant (56–58). Analyses were performed by a researcher blind to the experiment.

Downloaded from www.fasebj.org to IP 151.97.98.252. *The FASEB Journal* Vol., No. , pp:, November, 2016

Isolation and culture of brain macrophages/microglia

In brain injury, reactive microglia lose their characteristic ramified shape, express macrophage phenotypic markers, exhibit macrophage-like characteristics, and secrete a number of cytotoxic mediators, including NO (19–21). To investigate the effect of MPTP on macrophage/microglia NO production, Wt and GR-deficient mice were killed by quick decapitation at various times after saline or MPTP treatment, starting from 6 h after the first MPTP injection, as indicated. Brains were rapidly dissected under sterile conditions, and activated macrophages/microglia were isolated by means of adherence to plastic well, according to described previously methods (50, 61–63). The isolated adherent cells were collected and cultured in RPMI 1640, supplemented with 1 mM L-glutamine, 0.5% HEPES (Flow Laboratories Irvine, UK) penicillin G, (100 U/ml) streptomycin (100 μg/ml), and 10% heat-inactivated FCS, in 24-well plates at 37°C. Cells were immunoreacted for activated macrophage/microglial-specific (Mac-1/CD11b, major histocompatibility Class II MHC) and non-specific (GFAP for astrocyte, galactocerebroside, GAL-C, for oligodendrocyte, or neurofilament, NF, for neuron) markers. The cells were either cultured for 48 h alone or in the presence of lipopolysaccharide (LPS), as described (50). After 48 h the supernatants of the cells were collected for measurement of nitrites. Subsequently, the number of cells was determined after harvesting by trypsinization in Ca/Mg-free PBS and washing in RPMI media. Viability of the cells was determined by means of trypan blue exclusion. The nitrite content of the culture supernatant was corrected for the number of isolated cells afterwards.

GR binding capacity

GR binding capacity was evaluated in macrophage/microglial cultures isolated as above, at different time-intervals after MPTP treatment, as described previously in full details (40–44). Briefly, cells were harvested by scraping into Earl's balanced salt solution and washed twice. The pellet was resuspended in 1.5 volumes of 10 mM HEPES, 1 mM EDTA, and 10 mM sodium molybdate, pH 7.4, and ruptured with a Dounce homogenization. Homogenates were centrifuged at 105,000 × g for 45 min at 0°C. Binding to cytosolic GR was determined by incubation in duplicates with [^{3}H]dexamethasone (70 Ci/mmol; Amersham Pharmacia Biotech, Germany) at concentrations ranging from 0.5 to 40 nM for 20–24 h at 4°C. The amount of non-specific binding was determined in parallel incubations of the labeled steroid in the presence of 500-fold excess of the specific GR competitor, unlabeled RU 28362 (New England Nuclear-DuPont, Boston, MA). Sephadex-LH-20 (Pharmacia Biotech, Uppsala, Sweden) columns equilibrated with TEDGM buffer were used to separate bound from unbound steroid (40, 43). Radioactivity was counted in a Packard scintillation counter at 55% efficiency. Protein content was determined according to the method of Lowry (55) by using BSA as a standard. Specific binding calculated as the difference between total and non-specific binding (fentomoles of [^{3}H]dexamethasone bound per mg protein) are expressed as fmol/mg protein. Total binding (B_{max}) and binding affinity (K_d) were derived by Scatchard analysis (40, 43; Table 2).

Cell treatments

The effect of LPS (100 ng/ml) activation was studied either in the absence or the presence of the NO synthase (NOS) inhibitors; N(ω)-nitro-L-arginine methylester (L-NAME), N(g)-monomethyl-L-argine (L-NMMA), the inactive enantiomer N(g)monomethyl-D-arginine, the

Downloaded from www.fasebj.org to IP 151.97.98.252. *The FASEB Journal* Vol., No. , pp:, November, 2016

specific inhibitor of inducible NOS, (iNOS), L-N6-(1-iminoethyl)-lysine (L-NIL) (64, 65), at 2 μg to 2.0 mg/ml, or corticosterone at 10^{-11}–10^{-6} M. These studies were also performed in absence or presence of the GR antagonist Mifepristone, RU486 [(17β-hydroxy-11-β(4-dimethylaminophenyl)-17α(propynil)-estra-4,9-dien-3-one) at a concentration of 10^{-6} M (kindly provided by Roussel Uclaf, Hoechst, France). After 24 h, the supernatants were collected for nitrite analysis.

Nitrite assay

The production of NO, as measured by the formation of the stable decomposition product nitrite, was determined in cell-free supernatant (50). Briefly 100 μl of supernatant was mixed with 100 μl Griess reagent [1% sulfanilamide plus 0.1% N-(1)naphtylethylenediamine in 2.5% H_3PO_4]. After 10 min at RT, the optical density at 540 nm was measured. In parallel, a sodium nitrite standard curve (1–200 μM) was generated. Samples were tested in triplicate and results represent the mean ± SE. of at least six mice/group.

L-NIL oral administration

To examine the effect of iNOS inhibition in vivo during the early phase of MPTP treatment, Wt and GR-deficient mice were given the specific iNOS inhibitor, L-NIL.

L-NIL was added to the drinking water (100 μg/ml; 50, 66) starting 24 h before the first MPTP injection and continuing for 10 consecutive days. Solutions were prepared daily, fluid consumption in both L-NIL treated and untreated mice was monitored due to possible changes in water consumption, and doses of L-NIL were adjusted accordingly (50, 66). Groups of healthy Wt and Tg mice received L-NIL for 10 consecutive days. On Day 7 after MPTP discontinuance, groups of saline and L-NIL treated mice were anesthetized and perfused as above, and the brains were post-fixed and cryoprotected for TH immunocytochemistry (five mice/group). Part of the mice (six mice/group) were killed by quick decapitation, and the left and right striatum were rapidly dissected and processed for high-affinity dopamine up-take. Isolation and processing of brain macrophages/microglia was performed in groups (six mice/group) of saline- and L-NIL-treated mice and nitrite production measured in supernatants as described.

Statistical analysis

Data were analyzed by means of two-way ANOVA (ANOVA), with group and time as independent variables and given as mean ± SE. Striatal neurochemical data were expressed in nanomoles or picomoles per milligram per protein. Comparisons a posteriori between different experiments were made by Student-Newman-Keuls *t*-test.

RESULTS

Lifelong GR deficiency exacerbates MPTP-induced toxicity to dopaminergic neurons

Time-dependent changes of striatal neurochemical parameters

One day After MPTP discontinuance, striatal dopamine, DOPAC, and HVA levels had significantly decreased in both Wt and Tg mice, as compared with controls. However, decreases in GR-deficient mice were significantly greater than their Wt counterparts. Hence, striatal

Downloaded from www.fasebj.org to IP 151.97.98.252. *The FASEB Journal* Vol., No. , pp:, November, 2016

dopamine, DOPAC, and HVA levels had reduced by 68, 53, and 38%, compared with 85, 66, and 50% in GR-deficient mice, respectively (Fig. 1*A–C*). Consequently, striatal (DOPAC+HVA)/dopamine ratio**,** which is a reliable index of DA turnover, had significantly increased in GR-deficient compared with Wt (Fig, 1*E*). 3-MT levels, which can be assumed to be an index of dopamine release (67), had significantly decreased by ~40% in both Wt and GR-deficient mice (Fig. 1*F*). However, the latter had basal levels of 3-MT significantly lower (by ~26%) than Wt counterpart. In contrast, 5-HT (Fig. 1*D*) and 5-HIAA levels (data not shown) were in the range of the control values in both GR-deficient and Wt mice. Ascorbic acid levels were unaffected in both GR-deficient and Wt mice (Fig. 2*A*), whereas DHAA had significantly increased by ~57% (Fig. 2*B*), with a consequent increase by ~64% in the DHAA/ascorbic acid ratio (Fig. 2*C*). Ascorbic acid has been proposed recently as an ultimate neuronal sink for radicals generated during metabolic activity of the nigro-striatal dopaminergic system (40). In addition, the DHAA/ascorbic acid ratio can be assumed as a reliable index of the ascorbic oxidative status and reactive oxygen species (ROS) formation (68). Thus, the increase in the DHAA/ascorbic acid ratio only in GR-deficient mice indicates an early increase in the ascorbic acid oxidative status, most likely as a consequence of increased ROS generation.

Seven days after MPTP discontinuance

At this time point, decreases in striatal dopamine (66%), DOPAC (58%), and HVA (41%) in Wt mice were in the range of those of Day 1, as opposed to GR-deficient mice exhibiting a further reduction (by 92, 83, and 67%, respectively; Fig. 1*A–C*). The (DOPAC+HVA)/DA ratio in Wt mice was still in the range of control values, as opposed to GR-deficient mice exhibiting a further (sixfold) increase, compared with controls Fig. 1*E*). In addition, 3-MT levels showed a significant trend to recovery ($P<0.05$, compared with Day 1 values) in Wt; in contrast, a further significant decrease (by ~62%) was measured in Tg mice (Fig. 1*F*). These findings denote a recovery of dopaminergic functioning in Wt mice, because 3-MT level can be assumed to be a reliable index of DA release (67). Ascorbic acid and DHAA levels were still unmodified in Wt mice (Fig. 2*A–B*). By contrast, in GR-deficient mice, the slight reduction of ascorbic acid coupled with the sharp increase in DHAA levels resulted in a sharp increase of DHAA/ascorbic acid ratio (Fig. 2*C*).

Eleven days after MPTP discontinuance

Dopamine (decreases by ~60%), DOPAC (decreases by ~38%), and HVA (decreases by ~30%) levels in Wt mice showed a trend toward a recovery, as compared with Day 7. Recovery for DOPAC levels reached statistical significance (Fig. 1*A–C*). In GR-deficient mice, decreases in dopamine (85%), DOPAC (64%), HVA (58%), and 3-MT (37%) levels were still marked, although the recovery for DOPAC and 3-MT levels reached statistical significance, compared with Day 7 (Fig. 1*A–C*, *F*). Both (DOPAC+HVA)/DA (Fig. 1*E*) and DHAA/ascorbic acid (Fig. 2*C*) ratios in Tg mice were significantly decreased, as compared with Day 7 values; however, DHAA/ascorbic acid ratio was still significantly higher than Wt mice, denoting a long-lasting up-regulation of ROS production as a result of the GR deficiency.

GR-deficient mice fail to recover from MPTP-induced dopaminergic neurotoxicity

To assess the ability of Wt and GR-deficient mice to recover following MPTP-exposure, high-affinity synaptosomal up-take, which is a reliable quantitative indicator of dopaminergic axonal

Downloaded from www.fasebj.org to IP 151.97.98.252. *The FASEB Journal* Vol., No. , pp:, November, 2016

terminal density, was determined at different time-points (1–7–11–21 days) after a single MPTP 55 mg/kg injection (Fig. 3). One day after MPTP, striatal dopamine up-take in Wt mice had decreased to 64% of control, whereas the decrease (46% of controls) in GR-deficient mice was significantly greater ($P<0.01$). A further reduction in dopamine up-take levels was observed on Day 7, although a greater inhibition was measured in GR-deficient mice (24% of control) compared with their Wt counterparts (50% of control, $P<0.01$). By Day 11, dopamine up-take showed a trend to increase in Wt mice (58% of control), whereas a marked reduction (36%) was still measured at this time point in GR-deficient mice (Fig. 3). By Day 21, Wt mice showed a significant trend toward a recovery of the dopaminergic terminals functioning, as revealed by the significant increase in dopamine up-take (77% of control). By contrast, dopamine up-take was still significantly reduced (40% of control) in GR-deficient mice.

Endogenous GC levels are similarly elevated in Wt and GR-deficient mice in response to MPTP

GCs have been reported to compromise the neuronal ability to survive necrotic insults (2, 3). Because Tg mice exhibit aberrant HPA axis response to stress (40–49), it was important to verify the endogenous levels of plasma corticosterone in response to MPTP. As observed in Table 1, Wt and GR-deficient mice given saline had similar levels of corticosterone. Following MPTP, Wt and Tg mice exhibited a marked and sustained plasma corticosterone response; the peak occurred at Day 7, and corticosterone levels returned to nearly saline-groups values 21 days after MPTP discontinuance (Table 1).

GR-deficiency exacerbates loss of tyrosine hydroxylase-immunoreactive (TH-IR) cell bodies with no recovery

TH is the rate-limiting enzyme in dopamine biosynthesis and a marker for dopaminergic neurons. To evaluate MPTP effects on dopaminergic cell bodies in Wt and GR-deficient mice, we assessed midbrain sections (at the level of the dopaminergic cell bodies in the SN) immunostained with TH antiserum. In female B6C3F1 controls (C57B × C3H), TH immunocytochemistry revealed no significant difference in the number of TH-IR neurons (revealed by CY3, in red), between Wt and GR-deficient in SN (Fig. 4*A–C*). By contrast, one day after MPTP discontinuance, GR-deficient mice showed a reduction of ~60% in TH-IR neurons in the SN, in contrast with Wt mice, which had an approximate 30% depletion (Fig. 4*B*, *D–E*). Seven days after MPTP discontinuance, Wt mice showed an approximate 60% depletion of TH-IR neurons, whereas GR-deficient mice exhibited an almost 80% loss, compared with Wt or Tg saline-injected controls (Fig. 4*B*, *F–G*). In Wt mice, starting from Day 11, a trend toward a slight recovery was observed (Fig. 4*B*) and by twenty-one days after MPTP discontinuance, a modest return of TH expression was observed in SN (Fig. 4*B*), indicating that a certain number of dopaminergic neurons could survive the MPTP insult, as reported by other investigators (see, 38). By contrast, in GR-deficient mice, such trend toward a recovery was less apparent, and a marked loss of TH-IR cell bodies was still observed at either 11 and 21 days after MPTP discontinuance (Fig. 4*B*, *H–I*).

Downloaded from www.fasebj.org to IP 151.97.98.252. *The FASEB Journal* Vol., No. , pp:, November, 2016

GR-deficiency increases glial hypertrophy and glial inducible nitric oxide synthase (iNOS) immunoreactivity in response to MPTP

To investigate whether differences in glial response to MPTP might contribute to the increased vulnerability of GR-deficient mice, striatal, and nigral sections were reacted at various times after the lesion with antibodies to GFAP, iNOS, and Mac-1. In both Wt and GR-deficient mice, immunolabeling for GFAP was sharply increased in the striatum (not shown) and midbrain as early as one day after MPTP. Double-labeling of GFAP-IR (revealed by FITC, in green) astrocytes and TH-IR (revealed by CY3, in red) neurons in SN revealed a greater astrocyte invasion in GR-deficient compared with Wt mice at all times tested following MPTP discontinuance (Fig. 5*A–F*). In addition, in GR-deficient SN, hypertrophic GFAP-IR astrocytes had enlarged cell bodies (Fig. 5*D*, *F*, *H*, inserts) with processes surrounding the fewer TH-IR neurons (Fig. 5*F*, *H*, inserts). Maximal astroglia activation in the striatum (not shown) and midbrain of GR-deficient mice occurred earlier (1 day) than Wt mice, in which peak changes were observed 7 days after MPTP. By 11 days, increases of GFAP-IR cells were still observed in striatum and midbrain of Wt mice (not shown), while by 21 days hypertrophy of astrocytes was reduced, and numerous surviving TH-IR neuronal cell bodies were localized within GFAP-IR processes (Fig. 5*G*, inserts). In GR-deficient mice, GFAP-IR hypertrophic astrocytes appeared reduced but remained distributed in the striatum and midbrain at both 11 (not shown) and 21 days after MPTP discontinuance (Fig. 5*D*, *F*, *H*). iNOS immunoreactivity in striatum and SN did not revealed differences between saline-injected Wt and Tg mice. However, as early as 1 day after MPTP, a strong immunofluorescent iNOS signal (revealed by FITC in green) was localized in the SN of Tg (Fig. 6*B*) compared with Wt (Fig. 6*A*) mice. Two morphologically different cell types were stained by iNOS in the SN of Tg mice: (1) process-bearing GFAP-IR astrocytes (Fig. 6*B*, arrows and insert), and (2) GFAP-negative round- to oval-shaped cells (Fig. 6*B*, arrowhead). Fusion of confocal microscopic images revealed extensive overlap of GFAP and iNOS markers in astrocytic cell bodies, nuclei, and processes (Fig. 6*B*, arrows and insert) of Tg, whereas a weaker signal was identified in GFAP positive (Fig. 6*A*, insert) and negative cells (Fig. 6*A*, arrowhead) of Wt mice. When adjacent nigral sections were stained for the prototypic marker of activated macrophage/microglia, Mac-1/CD11b (revealed by CY3, in red), numerous Mac-1 cells were localized in the SN of Tg (Fig. 6*D*) compared with Wt (Fig. 6*C*) mice SN. When double labeling was performed for iNOS and Mac-1, fusion of confocal microscopic images revealed extensive overlap of Mac-1 and iNOS in both Wt and GR-deficient SN (Fig. 6*C–D*, inserts. Accordingly, an intense nitrotyrosine (NT) immunofluorescent reaction was revealed in TH-IR neurons of GR-deficient SN, as opposed to NT reaction observed in Wt TH-IR neurons (not shown).

GR-deficiency induces aberrant macrophage/microglia iNOS/NO response to MPTP, which precedes dopaminergic neurotoxicity

Activated microglial cells, like all phagocytic cells, release short-lived cytotoxic factors, including NO, hydrogen peroxide, and superoxide radicals, which may exacerbate neuronal insult (17–21). The role played by macrophage/microglia iNOS/NO response (measured by its decomposition product nitrite) to MPTP neurotoxicity was next assessed at various time-intervals after MPTP, and GR binding capacity correlated. The cultured cells were immunoreactive for Mac-1/CD11b and were not immunoreactive for astrocyte, oligodendrocyte, or neuronal markers. In control Wt and GR-deficient mice, few cells were obtained with this

Downloaded from www.fasebj.org to IP 151.97.98.252. *The FASEB Journal* Vol., No. , pp:, November, 2016

method (~1.0 ± 0.2 × 10^5 cells/brain), as was described previously (63). From these cells no measurable spontaneous NO production could be detected. In contrast, from the brains of MPTP-treated mice, the number of isolated macrophages/microglia increased, expressed iNOS, and released various amount of NO (Fig. 7*A–C*). GR-deficient CNS phagocytes exhibited strong iNOS immunofluorescent signal (Fig. 7*A*) and produced three- to fourfold higher nitrite levels compared with their Wt counterparts (Fig. 7*B*). Thus, by 6 h after the first MPTP injection, GR-deficient microglia produced NO (3.9 ± 0.7 μM/10^5 cells) 3 times Wt microglia (0.9 ± 0.3 μM/10^5 cells; $P<0.01$). In addition, a further sharp increase in NO production occurred after 12 h, and a plateau was reached thereafter in GR-deficient mice (3.9 ± 0.7 μM), whereas in Wt mice nitrite levels increased to a lesser extent at either 12 (1.5 ± 0.5 μM) or 24 h (2.6 ± 0.6 μM). One day after MPTP discontinuance, GR-deficient macrophage/microglia produced almost 2 times more nitrites when compared with their Wt counterparts (Fig. 7*B*) ($P<0.01$). These levels were still 2–3 times higher 7–11 days after MPTP discontinuance. By day 21, nitrite levels had decreased by almost 50% in either Wt or Tg mice; however, NO levels were still fourfold higher in GR-deficient mice (Fig. 7*B*; $P<0.01$).

The analysis of GR-B data in cultured microglia indicated a significant alteration in the kinetics of GR-B in Tg compared with Wt mice (Table 2). Scatchard analysis of the data indicated a sharp decrease in the B_{max} (total number of binding sites) in Tg as compared with Wt cultures at all time tested (Table 2). Thus, 12 h after MPTP, GR-deficient microglia exhibited a marked loss of GR-B, compared with Wt mice ($P<0.01$), and a further and long-lasting loss of GR-B capacity was measured during all the experimental protocol. By contrast, in Wt cultures, GR-B capacity decreased to a lesser extent by 1 day after MPTP, while by 7–11 days, those levels significantly increased to reach control values by 21 days (Table 2; $P<0.01$). The K_d values (binding affinity) were slightly increased in activated macrophage/microglial cultures after MPTP, indicating a tendency toward reduced GR binding affinity in Tg-deficient cells.

GR-deficient macrophage/microglia are resistant to NO inhibition by GCs

GR expression and binding have been documented in astrocytes, macrophages, and microglia, and GCs are known inhibitors of iNOS/NO in these systems (7, 8, 50, 69–71). We therefore investigated the capability of GCs to regulate NO production by macrophages/microglia cultures from brains of Wt and Tg mice 7 days after MPTP discontinuance, compared with direct inhibition by NOS inhibitors. Stimulation by LPS induced a significant increase in NO generation in both Wt and Tg mice. However, LPS induced an almost twofold increase in GR-deficient as compared with Wt mice (Fig. 7*C*). The LPS-induced production of nitrites was suppressed by L-NAME, L-NMMA (data not shown), and L-NIL (Fig. 7*C*) in both Wt and Tg mice. However, L-NIL was ~10- to 50-fold more potent, with an IC_{50} (dose required to suppress nitrite formation by 50%) of 10 μM, as compared with L-NMMA (110 μM) or L-NAME (800 μM), whereas the inactive enantiomer of L-NAME, N(g)monomethyl-D-arginine, was without effect (not shown). These findings clearly support the hypothesis that iNOS activation was responsible for higher nitrite formation of Tg microglia. Administration of corticosterone to LPS-stimulated microglia induced a dose-dependent inhibition of NO formation in cultures from Wt mice, with an IC_{50} of 9.7 × 10^{-9} M, and a complete prevention of NO formation at 10^{-7} M. This effect was mediated by GRs, because pretreatment with the GR-antagonist RU486 (10^{-6} M) completely counteracted corticosterone-induced inhibition of nitrite production (3.9 ± 0.6 μM after RU486, compared with 0.9 ± 0.05 μM in the absence of RU486). In cultures from GR-

Downloaded from www.fasebj.org to IP 151.97.98.252. *The FASEB Journal* Vol., No. , pp:, November, 2016

deficient mice, corticosterone failed to induce inhibition of NO formation (IC_{50} = 9.88 × 10^{-7} M). More importantly, corticosterone was unable to suppress NO formation even at the highest concentrations (10^{-6} M), whereas in the presence of L-NIL, NO levels were similarly suppressed in both Wt and Tg cultures.

Thus, in GR-deficient brain phagocytes, GRs are sharply down-regulated and the high production of nitrite levels was not suppressed by exogenous application of corticosterone. In addition, microglial sensitivity to corticosterone inhibitory effect was reduced.

iNOS inhibition counteracts increased vulnerability of GR-deficient mice to MPTP

To examine the relevance of iNOS/NO activation in the increased vulnerability of GR-deficient mice to MPTP, the specific iNOS inhibitor L-NIL was added to the drinking water for 10 consecutive days, starting 24 h before the first injection of MPTP, and mice were killed 7 days after MPTP discontinuation. This route of administration and the dose-regimen used were previously demonstrated to suppress peripheral nitrites production stimulated by immunization with myelin oligodendrocyte peptide (50). The administration of L-NIL to GR-deficient mice resulted in a significant attenuation of MPTP-induced toxic effects (increases in nitrite production and decreases in striatal high-affinity dopamine up-take); the changes in these parameters were identical to those observed in Wt counterparts. Thus, L-NIL induced a significant increase in striatal dopamine up-take in both Wt and GR-deficient mice, compared with MPTP-treated Wt and GR-deficient mice (Fig. 8*A*). In addition, L-NIL treatment suppressed both the up-regulated macrophage/microglial nitrite levels of MPTP-treated GR-deficient mice and the nitrite generation in Wt mice (Fig. 8*B*). Treatment with L-NIL reduced TH-IR neuronal cell loss in both Wt and GR-deficient mice (not shown). However, the administration of L-NIL alone did modify neither the number of TH-IR neurons, nor glial NO from cultures from either Wt or GR-deficient mice (not shown).

DISCUSSION

The key finding of this study is that early embryonic life expression of a defective GR in genetically modified mice programs a dramatic increase in the vulnerability of the nigro-striatal dopaminergic system to MPTP. Hence, loss of GR expression, binding capacity, and signaling were associated with an earlier, sharper, and longlasting impairment of a number of biochemical parameters of nigro-striatal dopaminergic functioning and with a significant increase in the oxidative and nitrosative status in the striatum and SN of GR-deficient mice. Endogenous GC levels were similarly increased, whereas immunocytochemical studies revealed a greater astroglial activation and iNOS expression in GR-deficient astrocytes and macrophages/microglial cells. In addition, in vitro studies indicated that a sharp increase in reactive nitrogen species production by activated macrophage/microglia preceded dopaminergic neurotoxic effects of MPTP in GR-deficient mice. Moreover, in vivo treatment of GR-deficient mice with the specific iNOS inhibitor L-NIL prevented glial-derived NO generation and counteracted MPTP-induced neurotoxic effects. In L-NIL treated GR-deficient mice, the neurotoxic effects of MPTP were comparable with those observed in L-NIL-treated Wt counterparts, thus supporting the indication that increased vulnerability was linked to excess in NO production as a result of the GR deficiency.

Downloaded from www.fasebj.org to IP 151.97.98.252. *The FASEB Journal* Vol., No. , pp:, November, 2016

The potential role of iNOS/NO in MPTP-induced neurotoxic processes has been described previously (27–34). The role of GCs as critical factors involved in increasing neuronal vulnerability to oxidative insults is also recognized (2–4). However, we herein demonstrate that protection from exacerbation of MPTP-induced dopaminergic neurotoxicity requires a functional GR to down-regulate astroglial inflammatory reaction and establish for the first time a direct link between GR, endogenous NO production, and MPTP vulnerability. In view of the critical role of NO in neuroendocrine-immune communications (72–74), it seems tempting to suggest iNOS-derived NO as a potential final common pathway in the HPA axis programming of dopaminergic neuron vulnerability to MPTP and to define activated astrocytes/macrophages/microglia as chief compartments involved in this phenomenon. The present data are strengthened by our previous studies using the same mice, demonstrating a critical role of macrophage-derived NO production in determining the sensitivity or resistance to induced experimental autoimmune encephalomyelitis (EAE), a model of multiple sclerosis (50). The fact that the same GR-deficiency that results in lack of glucocorticoid regulation of NO generation provides resistance to EAE via immunosuppression, but sensitivity to MPTP-induced parkinsonism via innate inflammatory mechanisms highlight the importance of an efficient HPA-immune dialogue via GR-NO cross talk in programming vulnerability to degenerative diseases of the CNS (Fig. 9).

In accordance with our recent study performed in male Swiss mice (39), MPTP intoxication led to a rapid and significant impairment of the striatal dopaminergic functioning in both Wt and Tg female B6C3F1 (C57BL female × C3H male) mice. The depletion of striatal dopamine and 3-MT levels measured as early as one day following MPTP discontinuation, coupled with the increases in both (DOPAC+HVA)/ dopamine) and DHAA/ascorbic acid ratios in GR-deficient far greater than in Wt mice, indicate oxidative stress as one potential factor responsible for the increased vulnerability of the Tg mice (39, 67). In fact, dopamine oxidative metabolism represents a known mechanism of ROS generation because enzymatic oxidation of dopamine generates H_2O_2 (39, 68). Our previous studies demonstrated that in MPTP-induced decrease in striatal dopamine levels, time-course changes in the ascorbic acid oxidative status paralleled that of both dopamine and hypoxanthine/xanthine oxidative metabolisms (39). Moreover, MPTP-induced decreases in striatal gluthatione levels were coupled with increases in DHAA and glutamate levels (39), thereby suggesting an impairment of glutamate-ascorbate hetero-exchange mechanism (75), which is considered to be an important brain neuroprotective mechanism (76). In accordance with these and other previous findings (see, 39), the MPTP-induced increase in ascorbic oxidative status in Tg far greater than in Wt mice, suggests an earlier impairment of the mechanisms ensuring the required (10 mM) neuronal ascorbic acid concentration (76), with a consequent deficiency of such protective mechanism at a critical time during MPTP intoxication (39). Indeed, unlike Wt mice, early MPTP-induced impairment of striatal dopaminergic functioning in Tg mice was associated with an earlier and greater loss of TH-IR neurons in SN, indicating that expression of a dysfunctional GR from early embryonic life can program an increased vulnerability of the nigro-striatal dopaminergic system to MPTP. Such hypothesis is supported by the finding of a decrease in the high-affinity synaptosomal dopamine up-take in GR-deficient mice earlier and a greater decrease than in Wt mice. The high-affinity synaptosomal dopamine up-take is a reliable and highly sensitive and quantitative parameter of dopaminergic terminal axon density (38).

The question, therefore, arises as to the mechanism(s) involved in earlier and greater loss of dopaminergic functioning in GR-deficient mice. Glial cells play crucial roles in the brain

Downloaded from www.fasebj.org to IP 151.97.98.252. *The FASEB Journal* Vol., No. , pp:, November, 2016

response to neuronal injury and plasticity (19–21, 38, 39). In addition, accumulating data clearly indicate that the activities of different hormones, including GCs, can have a major impact on astroglial cell function (4, 7, 8, 56, 58, 69–71, 77–80). Thus, a different response of the astroglial cell compartment of the GR-deficient mice might participate in this phenomenon. Hence, as early as one day after MPTP discontinuance, a greater activation of astrocytes and macrophage/microglia, as revealed by GFAP and iNOS immunocytochemistry, was observed in GR-deficient SN and striatum. The increase in nitrotyrosine-IR signal in GR-deficient TH-IR neurons greater than in Wt mice, suggests increased nitrosative stress as candidate mediator of early TH-IR neuron loss and impairment of dopaminergic functioning, as a result of the GR deficiency; moreover, it indicates glia as the key compartment involved in this phenomenon.

It should be pointed out that injury to the brain elicits a sequence of morphological and biochemical events mediated by activated microglia, the intrinsic macrophage population of the brain (19–21). Indeed, activated microglial cells exhibit typical macrophage-like characteristics, express macrophage markers, become highly motile, move along chemotactic gradients, synthesize, and release an immense variety of soluble factors (including cytokines, chemokines, proteolytic enzymes, NO, ROS, and complement proteins), reveal strong phagocytic activity and execute cytotoxic attacks (19–21). In the present study, macrophage/microglial cells, isolated from GR-deficient mouse brains and expressing typical markers of activated macrophage/microglia, produced threefold higher nitrites one day after MPTP discontinuance, thereby supporting the indication that peroxynitrites might be involved in the precocious loss of TH-IR neurons in GR-deficient mice. In addition, up-regulation of reactive nitrogen oxide species started 6 h after the first MPTP injection, therefore preceding neuronal demise. The present results are consistent with the hypothesis that excessive nitrosative/oxidative stress via iNOS/NO and ROS generation in Tg accounts for the early and marked impairment of dopaminergic functioning following MPTP exposure.

Indeed, high local concentrations of NO can combine with molecular oxygen to form reactive oxygen nitrogen species, such as N_2O_3. N_2O_3 can transfer NO^+ equivalent to nucleophilic sites in a reaction known as nitrosation (see, 81). Enzymes containing cysteine-zinc finger motifs, or reduced cystil residues at key sites, are susceptible to nitrosation-mediated inhibition (see, 82, 83). In fact, nitrosative stress and NO have been reported to inhibit dopamine-β-hydroxylase activity (81). In addition, MPTP has been shown to induce selective nitration of TH (39). By contrast, mice overexpressing copper/zinc superoxide dismutase are protected from striatal TH nitration, suggesting an important role of superoxide radicals in TH nitration and consequent loss of activity. It seems important to mention that reaction of NO with sulphydril groups yielding S-nitrosothiols may nitrosylate critical Cys residues of the GR (82–85), with consequent inhibition of GR binding activity and signaling [Fig. 7*A–C*, Table 2, (50, 85)]. Thus, a dysfunctional GR can program an abnormal response of astrocytic and macrophage/microglia compartments to MPTP-induced neuroinflammation, thereby resulting in aberrant production of cytotoxic nytrosil radicals, which in turn are responsible for neuronal damage (Fig. 9).

Indeed, specific GRs are expressed in astrocytes, macrophages, and microglial cells; GCs are potent inhibitors of iNOS-derived NO in these cell systems (4, 7, 8, 50, 69, 71) and have been shown to reduce ameboid microglial cell number and activity in vivo and in vitro (80). Although not addressed in the present study, the inhibition of iNOS/NO by GC-bound GR is consistent with the ability of GR to inhibit NFkB-mediated transcription of iNOS gene, by GC-induced

Downloaded from www.fasebj.org to IP 151.97.98.252. *The FASEB Journal* Vol., No. , pp:, November, 2016

increase in Ik-B protein levels, or through protein–protein interactions between GR and NFk-B, thereby inhibiting interaction of the latter with iNOS promoter and preventing the induction of iNOS transcription (13–15). Hence, a functional knockout of GRs at a critical time during central nervous system (CNS) inflammation might prevent the endogenous GC "protective" response, thereby resulting in aberrant inflammatory cascades (7, 8, 47, 50, 86; Fig. 9). The transient down-regulation followed by a recovery of GR-B capacity herein reported in Wt mice microglial cultures is consistent with this suggestion. Hence, on the one hand, GR-deficient macrophage/microglia appeared resistant to GC inhibition, because corticosterone (either endogenous or exogenous) could not to suppress LPS-stimulated NO production, whereas in Wt mice a similar dose of corticosterone significantly suppressed nitrite production. On the other hand, the failure of Tg mice to exhibit a more sustained corticosterone response to MPTP in the face of GR down-regulation appears reminiscent of their failure to exhibit a more robust plasma corticosterone response to stress, exogenously administrated CRH, acute IL-1 challenge, or MOG-immunization, compared with their Wt counterparts (41, 44, 45, 50) and suggest the participation of NO in this phenomenon (7, 8, 72–74). The inverse correlation between up-regulation of NO and decreased GR-B capacity of Tg mice cultures may suggest that increased iNOS/NO generation after MPTP first injection may contribute to the further lowering of GR expression and GR signaling. Then, the GR-deficiency may prime macrophage/microglial cells to produce higher amounts of NO via iNOS induction, either directly or through increased production of pro-inflammatory cytokines (7, 10, 50). Our data argue that an excess of NO production can trigger a feedback loop involving loss of GR signaling thus perpetrating or exacerbating NO output at a critical time during MPTP intoxication, resulting in hyper-induction of reactive nitrogen oxide species and a consequent damage of nigral neuron cell bodies. Consistent with this suggestion, oxidative stress-induced increase in cytokine expression has been associated with a reduction of GC responsiveness, both in vitro (50, 86, 87) and in vivo (88), whereas mice having increased GR gene dosage show enhanced in vivo resistance to stress and endotoxic shock (89). It is therefore feasible that GR down-regulation may also play a pivotal role in NO generation of Tg mice (50).

The relevance of iNOS/NO activation in the increased vulnerability of GR-deficient mice to MPTP was further demonstrated, in vivo, by treatment of GR-deficient mice with the specific iNOS inhibitor L-NIL. The prevention of macrophage/microglia NO production and counteraction of MPTP-induced neurotoxicity, which in Tg mice was identical to Wt mice, supported the indication that increased vulnerability was linked to the increased NO production as a result of the GR deficiency. The present study, however, does not allow conclusions as to whether, besides iNOS/NO, other factors play additional roles in MPTP neurotoxicity of GR-deficient mice. In addition, it remains to be determined whether GR-deficient nigrostriatal neurons, per se, are more vulnerable to oxidative /nitrosative stress.

In conclusion, this work identifies a novel link between GR and iNOS/NO in MPTP-induced experimental parkinsonism and defines macrophage/microglial cells as key mediators of increased vulnerability of dopaminergic neurotoxicity in GR deficient mice. In view of the early embryonic life GR gene expression in neuronal structure primordial including the basal ganglia (90), it seems tempting to speculate that prenatal experiences known to influence the expression and function of GRs by "programming" the response of astroglial cells to inflammatory stimuli, may influence the vulnerability to degenerative disorders of the CNS. These findings may have

Downloaded from www.fasebj.org to IP 151.97.98.252. *The FASEB Journal* Vol., No. , pp:, November, 2016

clinical implications for the development of neurodegenerative diseases in humans and may have important therapeutic implications for such neurodegenerative diseases.

ACKNOWLEDGMENTS

The authors wish to thank the Italian Ministry of Health (Strategic Research Project RF-2002, conv. n. 189), Italian Ministry of Research (MURST), OASI (IRCCS) Institution for Research and Care on Mental Retardation and Brain Aging Troina (EN) Italy, and The Medical Research Council of Canada for support of this project. M.C.M. and P.A.S. share the first authorship.

REFERENCES

1. De Kloet, E. R., and Reul, J. M. (1987) Feedback action and tonic influence of corticosteroids on brain function: a concept arising from the heterogeneity of brain receptor systems. *Psychoneuroendocrinology* **12,** 83–105

2. Mc Ewen, B. S. (1998) Protective and demaging affects of stress mediators. *N. Engl. J. Med.* **338,** 171–179

3. Sapolsky, R.M., Romero, L.M. and Munk, A.U. How do glucocorticoids influence the stress responses? Integrating, permissive, suppressive, stimulatory, and preparative actions.(2000) Endocr. Rev. 21, 55-89.

4. Nichols, R. N., Zieba, M., and Bye, N. (2001) Do glucocorticoids contribute to brain aging? *Brain Res. Rev.* **37,** 273–284

5. McEwen, B. S., Biron, C. A., Brunson, K. W., Bulloch, K., Chambers, W. H., Dhabar, F. S., Goldfarb, R. H., Kitson, R. P., Miller, A. H., Spencer, L.R.J., and Weiss, J. M. (1997) The role of adrenocorticoids as modulators of immune function in health and disease: neural, endocrine and immune interactions. *Brain Res. Rev.* **23,** 79–133

6. Chrousos, G. P. (2000) The stress response and immune function: Clinical implications. *Ann N.Y. Acad. Sci. USA* **917,** 38–67

7. Marchetti, B., Morale, M. C., Testa, N., Tirolo, C., Caniglia, S., Amor, S., Dijkstra, C. D., and Barden, N. (2001) Stress, the immune system and vulnerability to degenerative disorders of the central nervous system in transgenic mice expressing glucocorticoid receptor antisense RNA. *Brain Res. Rev.* **37,** 259–272

8. Morale, M. C., Gallo, F., Tirolo, C., Testa, N., Caniglia, S., Marletta, V., Spina-Purrello, V., Avola, R., Caucci, F., Tomasi, C., et al. (2001) The neuroendocrine-immune circuitry: from neuron-glial interactions to function: focus on gender and HPA-HPG interactions on early programming of NEI system. *Immunol. Cell Biol.* **79,** 400–417

9. Barnes, P. J., and Adcock, I. (1993) Anti-inflammatory actions of steroids: molecular mechanisms. *Trends Pharmacol. Sci.* **14,** 436–441

Downloaded from www.fasebj.org to IP 151.97.98.252. *The FASEB Journal* Vol., No. , pp:, November, 2016

10. Bogdan, C. (1998) The multiplex function of nitric oxide in (auto)immunity. *J. Exp. Med.* **187,** 1361–1365

11. Scheinman, R. I., Cogswell, P. C., Lofquist, A. K., and Baldwin, A. S. (1995) Role of transcriptional activation of I kappa B alpha in mediation of immunosuppression by glucocorticoids. *Science* **270,** 283–286

12. Auphan, N., DiDonato, J. A., Rosette, C., Helmerg, A., and Karim, M. (1995) Immunosuppression by glucocorticoids: inhibition of NF-kappa B activity through induction of I kappa B synthesis. *Science* **270,** 286–290

13. Jenkins, B. D., Pullen, C. B., and Darimont, B. D. (2001) Novel glucocorticoid receptor coactivator effector mechanisms. *Trends Endocrinol. Metab.* **12,** 122–126

14. Kleinert, H., Euchenhofer, C., Ihrig-Biedert, I., and Forsterman, U. (1996) Glucocorticoids inhibit the induction of nitric oxide II by down-regulating cytokine-induced activity of transcription factor nuclear-factor kappa B. *Mol. Pharmacol.* **49,** 15–21

15. De Vera, M. E., Taylor, B. S., Wang, Q., Shapiro, R. A., Billiar, T. R., and Geller, D. A. (1997) Dexamethazone suppresses iNOS gene expression by up-regulating I-kBα and inhibiting NF-KB. *AJP Gastrointest. Liver Physiol.* **273,** G1290–G1296

16. McGeer, E. G. and McGeer, P. L. Neurodegeneration and the immune system. (1995) In *Neurodegenerative Diseases* (Calne, D. B. Ed.), Chapter 18, pp. 277–300, W.B. Saunders Company, Philadelphia, London, Toronto

17. Jenner, P., and Olanow, C. W. (1996) Oxidative stress and the pathogenesis of Parkinson's disease. *Neurology* **47,** S161–S170

18. Kelian, T., and Drew, P. D. (2003) Effect of peroxisome proliferator –activated receptor-gamma agonists on central nervous system inflammation. *J. Neurosci. Res.* **71,** 315–325

19. Giulian, D. (1993) Reactive glia as rivals in regulating neuronal survival. *Glia* **71,** 102–110

20. Aloisi, F. (2001) Immune function of microglia. *Glia* **36,** 165–179

21. Streit, W. J. (2002) Microglia as neuroprotective, immunocompetent cells of the CNS. *Glia* **40,** 133–139

22. Tolwani, R. J., Jakowec, M. W., Petzinger, G. M., Green, S., and Waggie, K. (1999) Experimental models of Parkinson's disease: insights from many models. *Lab. Anim. Sci.* **49,** 363–371

23. Langston, J. W., Ballard, J. W., Tetrud, J. W., and Irwin, I. (1983) Chronic Parkinsonism in human due to a product of meperidine-analog synthesis. *Science* **219,** 979–980

24. Uhl, G. R., Javitch, J. A., and Snyder, S. H. (1985) Normal MPTP binding in parkinsonian substantia nigra: evidence of extraneuronal toxin conversion in human brain. *Lancet* **1,** 956–957

Downloaded from www.fasebj.org to IP 151.97.98.252. *The FASEB Journal* Vol., No. , pp:, November, 2016

25. Tipton, K. F., and Singer, T. P. (1993) Advances in our understanding of the mechanism of the neurotoxicity of MPTP and related compounds. *J. Neurochem.* **61,** 1191–1206

26. Iravani, M. M., Kashefi, K., Mander, P., Rose, S., and Jenner, P. (2002) Involvement of inducible nitric oxide synthase in inflammation-induced dopaminergic neurodegeneration. *Neuroscience* **110,** 49–58

27. Liberatore, G. T., Jackson-Lewis, V., Vukosavic, C., Mandir, A. S., Vila, M., McAuliffe, W. G., Dawson, V. L., Dawson, T. M., and Przedborski, S. (1999) inducibile nitric oxide synthase stimulates dopaminergic neurodegeneration in the MPTP model of Parkinson disease. *Nat. Med.* **5,** 1403–1409

28. Snyder, S. H. (1996) No NO prevents parkinsonism. *Nat. Med.* **2,** 965–966

29. Hantraye, P., Brouillet, E., Ferrante, R., Palfi, S., Dolan, R., Matthews, R. T., and Beal, M. F. (1996) Inhibition of neuronal nitric oxide synthase prevents MPTP-induced parkinsonism in baboons. *Nat. Med.* **2,** 1017–1021

30. Przedbborski, S., Jackson-Lewis, V., Yokojama, R., Shibata, T., Dawson, V. L., and Dawson, T. M. (1996) Role of neuronal nitric oxide in 1-methyl-4-phenyl-1,2,3,6-tetrahydropyridine (MPTP)-induced dopaminergic neurotoxicity. *Proc. Natl. Acad. Sci. USA* **93,** 4565–4571

31. Barthwal, M. K., Srivastava, N., and Dikshit, M. (2001) Role of nitric oxide in a progressive neurodegenration model of Parkinson's disease in the rat. *Redox Rep.* **6,** 297–302

32. Du, Y., Ma, Z., Lin, S., Dodel, R. C., Gao, F., Bales, R., Triarhou, L. C., Chernet, E., Perry, K. W., Nelson, D. L. G., et al. (2001) Minocycline prevents nigrostriatal dopaminergic neurodegeneration in MPTP model of Parkinsons disease. *Proc. Natl. Acad. Sci. USA* **98,** 14669–14674

33. Wu, D. C., Jackson-Lewis, V., Vila, M., Tieu, K., Teismann, P., Vadseth, C., Choi, D. K., Ischiropoulos, H., and Prezedborki, S. (2002) Blockade of microglial activation is neuroprotective in the 1-methyl-4-phenyl-1,2,3,6-tetrahydropyridine mouse model of Parkinson's disease. *J. Neurosci.* **22,** 1763–1771

34. Dehmer, T., Lindenau, J., Haid, S., Dichgans, J., and Schulz, J. B. (2000) Deficiency of inducible nitric oxide synthase protects against toxicity in vivo. *J. Neurochem.* **74,** 2213–2216

35. Levecque, C., Elbaz, A., Clavel, J., Richard, F., Vidal, J. S., Amouyel, P., Tzourio, C., Alperovitch, A., and Chartier-Harlin, M. C. (2003) Association between Parkinson's disease and polymorphism in the nNos and iNos genes in a community-based-case-control study. *Hum. Mol. Genet.* **12,** 79–86

36. Lapchak, P. A. (1998) A preclinical development strategy designed to optimize the use of glial cell line-derived neurotrophic factor in the treatment of Parkinson's disease. *Mov. Disord.* **13,** 49–54

Downloaded from www.fasebj.org to IP 151.97.98.252. *The FASEB Journal* Vol., No. , pp:, November, 2016

37. Tomac, A., Lindquist, E., Lin, L. F., Ogren, S. O., Young, D., Hoffer, B. J., and Olson, L. (1995) Protection and repair of the nigrostriatal dopaminergic system by GDNF in vivo. *Nature* **373,** 333–335

38. Ho, A., and Blum, M. (1998) Induction of interleukin-1 associated with compensatory dopaminergic sprouting in the denervated striatum of young mice: model of aging and neurodegenerative disease. *J. Neurosci.* **18,** 5614–5629

39. Serra, P. A., Sciola, L., Delogu, M. R., Spano, A., Monaco, G., Miele, E., Rocchitta, G., Miele, M., Migheli, R., and Desole, M. S. (2002) The neurotoxin 1-methyl-4-phenyl-1,2,3,6-tetrahydropyridine induces apoptosis in mouse nigrostriatal glia. Relevance to nigral neuronal death and striatal neurochemical changes. *J. Biol. Chem.* **277,** 34451–34461

40. Pépin, M. C., Pothier, F., and Barden, N. (1992) Impaired type II glucocorticoid-receptor function in mice bearing antisense RNA transgene. *Nature* **355,** 725–728

41. Stec, I., Barden, N., Reul, J. M., and Holsboer, F. (1993) Dexamethazone non-suppression in transgenic mice expressing antisense RNA to the glucocorticoid receptor. *J. Psychiatr. Res.* **28,** 1–5

42. Marchetti, B., Peiffer, A., Morale, M. C., Batticane, N., and Barden, N. (1994) Transgenic animals with impaired type II glucocorticoid receptor expression: a model to study aging of the neuroendocrine-immune system. *Ann. N.Y. Acad. Sci. USA* **719,** 308–327

43. Morale, M. C., Batticane, N., Gallo, F., Barden, N., and Marchetti, B. (1995) Disruption of hypothalamic-pituitary adrenocortical system in transgenic animals expressing type II glucocorticoid receptor antisense ribonucleic acid permanently impairs T cell function: effects on T-cell trafficking and T cell responsiveness during postnatal development. *Endocrinology* **136,** 3949–3960

44. Barden, N., Stec, I. S. M., Montkowski, A., Holsboer, F., and Reul, J. M. (1997) Endocrine profile and neuroendocrine challenge tests in transgenic mice expressing antisense-RNA against the glucocorticoid receptor. *Neuroendocrinology* **3,** 212–220

45. Karanth, S., Linthorst, A. C. E., Stalla, G. K., Barden, N., Holsboer, F., and Reul, J. M. (1997) Hypothalamic-pituitary-adrenocortical axis changes in a transgenic mouse with impaired glucocorticoid receptor function. *Endocrinology* **138,** 3476–3485

46. Sacedon, R., Vicente, A., Varas, A., Morale, M. C., Barden, N., Marchetti, B., and Zapata, A. (1999) Partial blockade of T-cell differentiation and marked alteration of the thymic microenvironment in transgenic mice with a dysfunctional glucocorticoid receptor function. *J. Neuroimmunol.* **98,** 1–167

47. Linthorst, A. C., Karanth, S., Barden, N., Holsboer, F., and Reul, M. H. (1999) Impaired glucocorticoid receptor function evolves in aberrant physiological responses to bacterial endotoxin. *Eur. J. Neurosci.* **11,** 178–186

Downloaded from www.fasebj.org to IP 151.97.98.252. *The FASEB Journal* Vol., No. , pp:, November, 2016

48. Linthorst, A. C., Flachskamman, C., Barden, N., Holsboer, F., and Reul, J. M. (2000) Glucocorticoid receptor impairment alter CNS responses to psychological stressors: an in vivo microdialysis study in transgenic mice. *Eur. J. Neurosci.* **12,** 283–291

49. Laflamme, N., Barden, N., and Rivest, S. (1997) Corticotropin- releasing factor and glucocorticoid receptor (GR) gene expression in the paraventricular nucleus of immune-challenged transgenic mice expressing type II GR antisense ribonucleic acid. *J. Mol. Neurosci.* **8,** 165–179

50. Marchetti, B., Morale, M. C., Brouwer, J., Tirolo, C., Testa, N., Caniglia, S., Barden, N., Amor, S., Smith, P. A., and Dijkistra, C. D. (2002) Exposure to a dysfunctional glucocorticoid receptor from early embryonic life programs the resistance to experimental autoimmune encephalomyelitis via nitric oxide-induced immunosuppression. *J. Immunol.* **168,** 5848–5859

51. Meaney, M. J., Diorio, J., Francis, D., Widdowson, J., La Plante, P., Caldji, C., Sharma, S., Seckl, J. R., and Plotsky, P. M. (1996) Early environmental regulation of forebrain glucocorticoid receptor gene expression: implications for the adrenocortical response to stress. *Dev. Neurosci.* **18,** 49–72

52. Bakker, J. M., Kavelaars, A., Kamphuis, P. J., Cobelens, P. M., van Vugt, H. H., van Bel, F., and Heijnen, C. J. (2000) Neonatal dexamethasone increases the susceptibility to experimental autoimmune diseases in adult rats. *J. Immunol.* **165,** 5932–5937

53. Shanks, N., Windle, R. J., Harbuz, M. S., Jessop, D. S., Ingram, C., and Lightman, S. M. (2000) Early–life exposure to endotoxin alters hypothalamic-pituitary-adrenal function and predisposition to inflammation. *Proc. Natl. Acad. Sci. USA* **97,** 5645–5650

54. Ahbon, E., Gogvadze, V., Chen, M., Celsi, G., and Ceccatelli, S. (2000) Prenatal exposure to high levels of glucocorticoids increase the susceptibility of cerebellar granule cells to oxidative stress-induced cell death. *Proc. Natl. Acad. Sci. USA* **97,** 14726–14730

55. Lowry, O. H., Rosembrough, N. J., Farr, A. L., and Randal, R. J. (1951) Protein measurement with the Folin reagent. *J. Biol. Chem.* **193,** 265–275

56. Gallo, F., Morale, M. C., Purrello, V., Tirolo, C., Testa, N., Farinella, Z., Avola, R., Baudet, A., and Marchetti, B. (2000) Basic fibroblast growth factor (bFGF) acts on both neurons and glia to mediate the neurotrophic effects of astrocyte on LHRH neurons in culture. *Synapse* **36,** 233–253

57. Gallo, F., Morale, M. C., Tirolo, C., Testa, N., Farinella, Z., Avola, R., Baudet, A., and Marchetti, B. (2000) Basic fibroblast growth factor priming increases the responsivenes of immortalized hypothalamic luteinizing hormone releasing hormone neurones to neurotrophic factors. *J. Neuroendocrinol.* **10,** 941–959

58. Avola, R., Spina-Purrello, V., Gallo, F., Morale, M. C., Marletta, N., Tirolo, C., Testa, N., Farinella, Z., and Marchetti, B. (2000) Immortalized hypothalamic luteinizing hormone-releasing hormone (LHRH) neurons induce a functional switch in the growth factor

Downloaded from www.fasebj.org to IP 151.97.98.252. *The FASEB Journal* Vol., No. , pp:, November, 2016

responsivennes of astroglia: involvement of basic fibroblast growth factor. *Int. J. Dev. Neurosci.* **18,** 743–763

59. Franklin, K. B. J., and Paxinos, G. (1997) The mouse brain in stereotaxic coordinates. Academic Press Inc. San Diego CA

60. Triarhou, L. C., Norton, J., and Ghetti, B. (1998) Synaptic connectivity of tyrosine hydroxylase immunoreactive nerve terminals in the striatum of normal, heterozygous and homozygous weaver mutant mice. *J. Neurocytol.* **17,** 221–232

61. Ruuls, S. R., Van der Linden, S., Sontrop, K., Huitinga, I., and Dijkstra, C. D. (1996) Aggravation of experimental allergic encephalomyelitis by administration of nitric oxide synthase inhibitors. *Clin. Exp. Immunol.* **103,** 467–476

62. de Groot, C. J., Hulshof, S., Hoozemans, J. J., and Veerhurs, R. (2001) Establishment of microglial cell cultures derived from postmortem human adult brain tissue: immunophenotypical and functional characterization. *Microsc. Res. Tech.* **54,** 34–39

63. de Groot, C. J., Sminia, T., and Dijkistra, C. D. (1989) Isolation and characterization of brain macrophages from the central nervous system of newborn and adult rats and of rats with experimental allergic encephalomyelitis. *Immunobiology* **179,** 314–327

64. Connor, J. R., Manning, P. T., Selle, S. L., Moore, W. M., Jerome, G. M., Webber, R. K., Tjoeng, F. S., and Cultre, M. G. (1995) Suppression of adjuvant-induced arthritis by selective inhibition of inducible nitric oxide synthase. *Eur. J. Pharmacol.* **273,** 15–19

65. McCartney-Francis, N. L., Song, X. Y., Mizel, D. E., and Wahl, S. M. (2001) Selective inhibition of inducible nitric oxide synthase exacerbates erosive joint disease. *J. Immunol.* **166,** 2734–2740

66. Willenborg, D. O., Fordham, S. A., Stakyova, M. A., Ramshaw, I. A., and Cowde, J. (1999) IFN-gamma is critical to the control of murine autoimmune encephalomyelitis and regulates both in the periphery and in the target tissue: a possible role for nitric oxide. *J. Immunol.* **163,** 5278–5286

67. Westerink, B. H. C., and Spaan, S. J. (1982) On the significance of endogenous 3-methoxytyramine for the effects of centrally acting drugs on dopamine release in the rat brain. *J. Neurochem.* **38,** 680–686

68. Noack, H., Lindenau, J., Rothe, F., Asayama, K., and Wolf, G. (1998) Differential expression of superoxide dismutase isoform in neuronal and glial compartment in the course of excitotoxically mediated neurodegeneration: relation to oxidative and nitrergic stress. *Glia* **23,** 285–297

69. Tanaka, J., Fujita, H., Matsuda, S., Toku, K., Masahiro, S., and Maeda, N. (1997) Glucocorticoid and minerlacorticoid receptors in microglial cells: two receptors mediate differential effects. *Glia* **20,** 1098–1136

Downloaded from www.fasebj.org to IP 151.97.98.252. *The FASEB Journal* Vol., No. , pp:, November, 2016

70. Drew, P. D., and Chavis, J. A. (2000) Female sex steroids: effects on microglial cell activation. *J. Neuroimmunol.* **111,** 77–85

71. Drew, P. D., and Chavis, J. A. (2000) Inhibition of microglial cell activation by cortisol. *Brain Res. Bull.* **52,** 391–396

72. McCann, S. M., Haens, G., Mastronardi, C., Walczewska, A., Karanth, S., Rettori, V., and Yu, W. H. (2003) The role of nitric oxide (NO) in control of LHRH release that mediates gonadotropin release. *Curr. Pharm. Des.* **9,** 381–390

73. McCann, SM. (1998) M., Kimura M., Karranth, S., Yu, W.H., and Rettori, V. (1998). Role of nitric oxide in the neuroendocrine responses to cytokines. *Ann. N. Y. Acad. Sci.* **840,** 174–184

74. S.M. McCann, M. Kimura, S. Karranth, W.H. Yu and V. Rettori (1997) Nitric oxide controls the hypothalamic-pituitary response to cytokines. Neuroimmunomodulation 4 (1997) 978-106.1997 Mar-Apr;4(2):98-106.

75. Miele, M., Bouteille, M., and Fillenz, M. (1994) The physiologically induced release of ascorbate in rat brain is dependent on impulse traffic, calcium influx and glutamate uptake. *Neuroscience* **62,** 87–91

76. Rice, M. E. (2000) Ascorbate regulation and its neuroprotective role in the brain. *Trends Neurosci.* **23,** 209–219

77. Bye, N., and Nichols, N. R. (1998) Adrenalectomy-induces apoptosis and glial responsiveness during aging. *Neuroreport* **9,** 1179–1184

78. Bye, N., Zieba, N. G., and Nichols, N. R. (2001) Resistance of the of the dentate gyrus to induced apoptosis during aging is associated with increase in transforming growth factor-beta1 messenger RNA. *Neurosceince* **105,** 853–862

79. Marchetti, B., Gallo, F., Farinella, Z., Tirolo, C., Testa, N., Caniglia, S., and Morale, M. C. (2000) Gender, neuroendocrine-immune interactions and neuron-glial plasticity. Role of luteinizing hormone-releasing hormone (LHRH). *Ann. N. Y. Acad. Sci.* **917,** 678–709

80. Wu, C. H., Chien, H. F., Chang, C. Y., Chen, S. H., and Huang, Y. S. (2001) Response of amoeboid and differentiating ramified microglia to glucocorticoids in postnatal rats: a lectin histochemical and ultrastructural study. *Neurosci. Res.* **40,** 235–241

81. Zhou, X., Espey, M.G., Chen, J.X., Hofseth, L.J., Miranda, K.M., Hussain- Pervez, S., Wink, D.A. and Harris, C.C. (2000) Inhibitory effects of nitric oxide and nitrosative stress on dopamine-beta-hydroxylase. *J. Biol. Chem.* **275,** 21241–21246

82. Arnelle, D., and Stamler, J. S. (1995) NO+, NO and NO- donation by S-nitrosothiols: implication for regulation of physiological functions by S-nitrosylation and acceleration of disulfide formation. *Arch. Biochem. Biophys.* **318,** 279–285

Downloaded from www.fasebj.org to IP 151.97.98.252. *The FASEB Journal* Vol., No. , pp:, November, 2016

83. Beckman, J. S., Chen, J., Ischiropoulos, H., and Crow, J. P. (1994) Oxidative chemistry of peroxynitrite. *Methods Enzymol.* **233,** 239–240

84. Simons, S. S. and Pratt, W. B. (1995) Glucocorticoid receptor thiols and steroid-binding activity. *Methods Enzymol.* **251,** 406–422

85. Galignana, M., Piwien-Pilipuk, G., and Assreuy, J. (1999) Inhbition of glucocorticoid receptor binding by nitric oxide. *Mol. Pharmacol.* **55,** 317–323

86. Ito, K., Lim, S., Caramori, G., Chung, K. F., Barnes, P. J., and Adcock, I. M. (2001) Cigarette smoking reduces histone deacetylase 2 expression, enhances cytokine expression, and inhibits glucocorticoid actions in alveolar macrophages. *FASEB J.* **15,** 1110–1112

87. Marchetti, B., Testa, N., Tirolo, C., Caniglia, S., Barden, N., and Morale, M. C. (2002) Glial-derived peroxynitrites mediate neurotoxicity in transgenic mice underexpressing glucocorticoid receptor (GR) antisense RNA from early embryonic life. 32RD Annual Meeting Soc. Neurosci., Miami. p. 1932

88. Cohen, J., and Glauser, M. P. (1991) Septic shock: treatment. *Lancet* **338,** 736–739

89. Reichard, H. M., Umland, T., Bauer, A., Kretz, O., and Schutz, G. (2000) Mice with an increased receptor gene dosage show enhanced resistance to stress and endotoxic shock. *Mol. Cell. Biol.* **20,** 9009–9017

90. Kitraki, E., Alexis, M. N., Papalopoulou, M., and Stylianopoulou, F. (1996) Glucocorticoid receptor gene expression in the embryonic rat brain. *Neuroendocrinology* **63,** 305–317

Received June 17, 2003; accepted October 1, 2003.

Downloaded from www.fasebj.org to IP 151.97.98.252. *The FASEB Journal* Vol., No. , pp:, November, 2016

Table 1

Effects of MPTP treatment on plasma corticosterone levels in Wt and GR-deficient mice

	Plasma corticosterone (ug/dl)				
Genotype	saline	MPTP + 1 d	MPTP + 7d	MPTP+ 11 d	MPTP + 21d
Wild-type	7.2 ± 0.9	25.3 ± 3.1*	31.4 ± 4.1*	26.0 ± 5.4*	15.4 ± 2.6*
GR-deficient	8.6 ± 1.7	18.6 ± 4.9*	25.6 ± 3.7*	19.5 ± 5.3*	11.9 ± 1.9

Plasma corticosterone was assayed, using a specific RIA (40, 43), in Wt and GR-deficient mice given saline (2 ml/kg) or MPTP (30 mg/kg intraperitoneally) for 5 consecutive days. The saline- and MPTP-treated groups were killed under stress-free conditions at the indicated time-intervals after MPTP discontinuance. *$P < 0.01$ vs. controls within each experimental group, respectively (ANOVA followed by Student-Neuman-Keuls post-hoc comparison).

Downloaded from www.fasebj.org to IP 151.97.98.252. *The FASEB Journal* Vol., No. , pp:, November, 2016

Table 2

Effects of MPTP treatment on GR binding capacity of macrophage/microglia cultures in Wt and GR-deficient mice

	K_d values	GR binding capacity (B_{max} fmol/mg protein)				
Genotype	(nM)	+12 h	+ 1 days	+ 7days	+ 11 days	+ 21 days
Wild-type	4.0 ± 0.6	70 ± 4	40 ± 3*	49 ± 4*	50 ± 5	65 ± 8
GR-deficient	6.8 ± 1.2	22 ± 3 *°	8 ± 2*°	7 ± 1*°	7 ± 1*°	12 ± 2*°

GR binding capacity (GR-B) was measured with [^{3}H]dexamethasone (40, 43). Cells were harvested by scraping into Earl's balanced salt solution and were washed twice and processed as described in Materials and Methods. Binding to cytosolic GR was determined by incubation in duplicates with [^{3}H]dexamethasone at concentrations ranging from 0.5 to 40 nM for 20–24 h at 4°C (40, 43). Specific binding was calculated as the difference between total and non-specific binding (fentomoles of [^{3}H]dexamethazone bound per mg protein). Total binding (B_{max}) and binding affinity (K_d) were derived by Scatchard analysis (40, 43). *$P < 0.01$ compared with 12 h, within each experimental group, respectively; ° $P < 0.01$ compared with Wt.

Downloaded from www.fasebj.org to IP 151.97.98.252. *The FASEB Journal* Vol., No. , pp:, November, 2016

Fig. 1

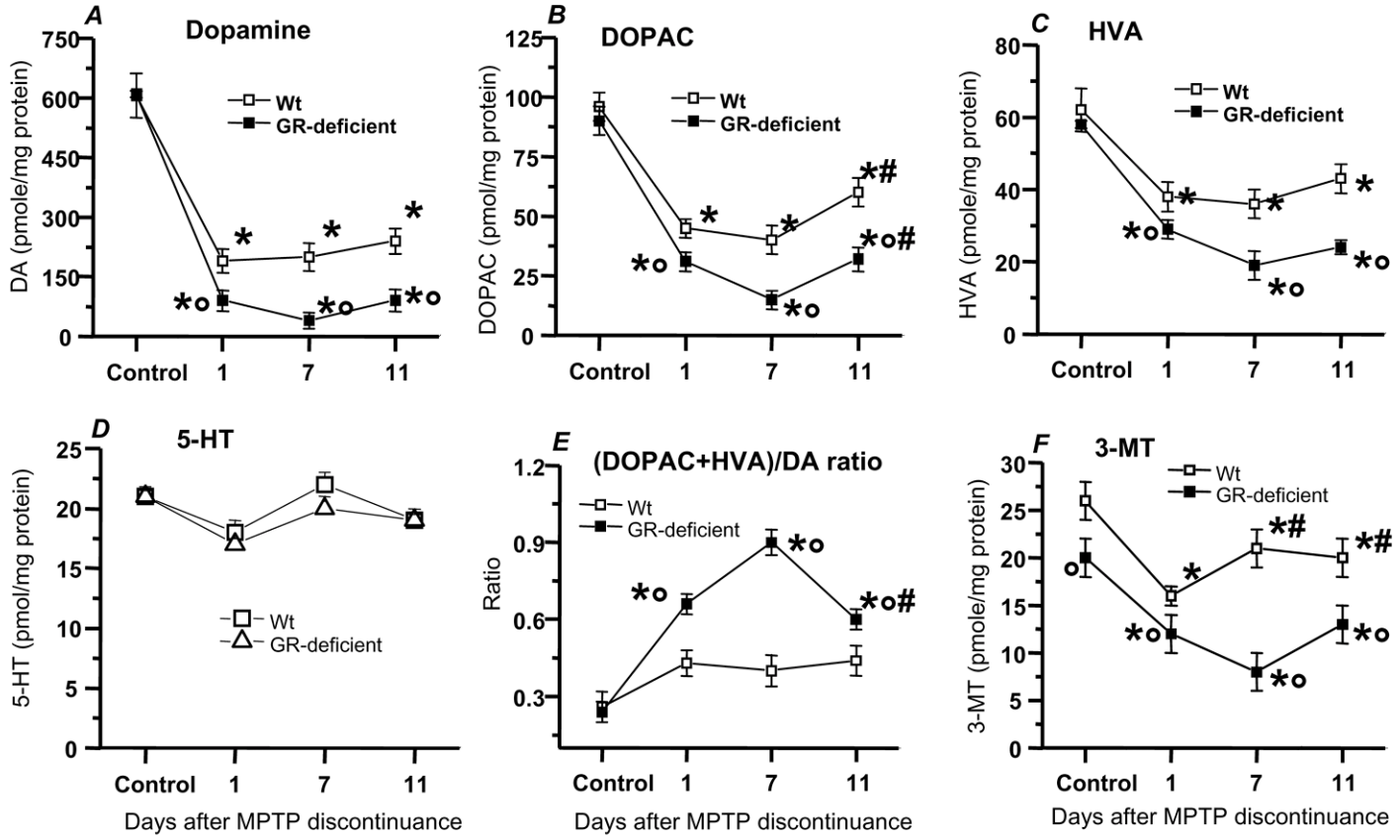

Figure 1. Levels of dopamine **(*A*)** DOPAC **(*B*)**, HVA **(*C*)**, 5-HT **(*D*)**, (DOPAC+HVA)/dopamine ratio **(*E*),** and 3-MT **(*F*)** in the striatum of Wt and GR-deficient mice at different days after MPTP discontinuance. Groups of eight Wt and GR-deficient mice per time period received intraperitonal injections of MPTP-HCl 30 mg/kg, at 24 h intervals, on 5 consecutive days. Mice were killed on the indicated days after MPTP discontinuance. Striatal neurochemicals determinations were performed by HPLC on pooled striata of both side. Values are given as mean ± SE $^{*}P < 0.01$ vs. controls (within each respective groups), $^{\#}P < 0.01$ vs. Day 7 or Day 1, and $^{\circ}P < 0.01$ vs. Wt (ANOVA followed by Student-Neuman-Keuls post-hoc comparison).

Downloaded from www.fasebj.org to IP 151.97.98.252. *The FASEB Journal* Vol., No. , pp:, November, 2016

Fig. 2

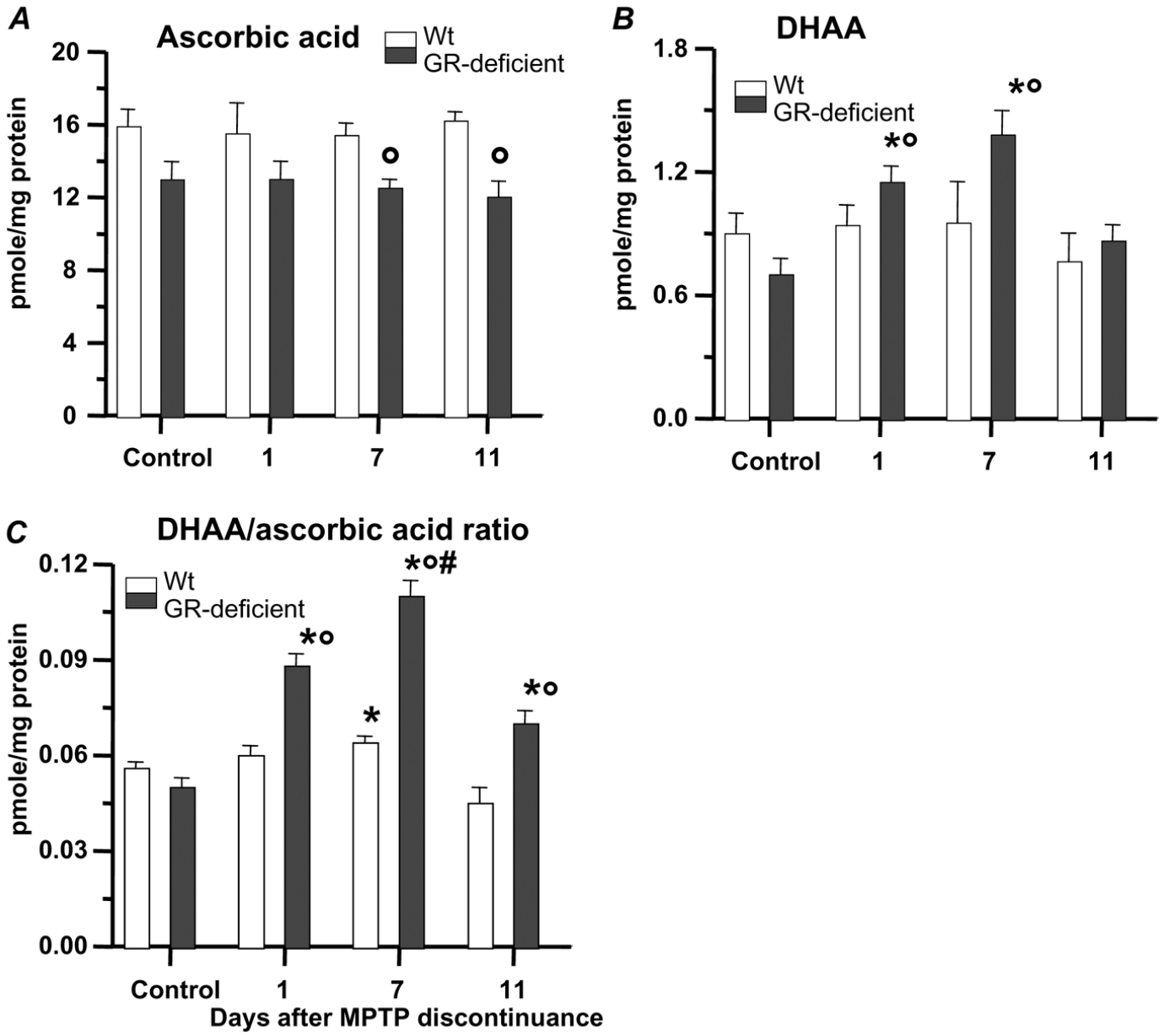

Figure 2. Levels of ascorbic acid **(*A*)**, DHAA **(*B*)**, and DHAA/ascorbic acid ratio **(*C*)** in the striatum of Wt and GR-deficient mice at different days after MPTP discontinuance. Groups of eight mice per time period received intraperitoneal injection of MPTP HCl 30 mg/kg, at 24 h intervals, on 5 consecutive days. Mice were killed on the indicated days after MPTP discontinuance. Striatal neurochemicals determinations were performed by HPLC. Values are given as mean ± SE *$P < 0.01$ vs. controls, $^{\#}P < 0.01$ vs. all time-points, and °$P < 0.01$ vs. Wt (ANOVA followed by Student-Neuman-Keuls post-hoc comparison).

Downloaded from www.fasebj.org to IP 151.97.98.252. *The FASEB Journal* Vol., No. , pp:, November, 2016

Fig. 3

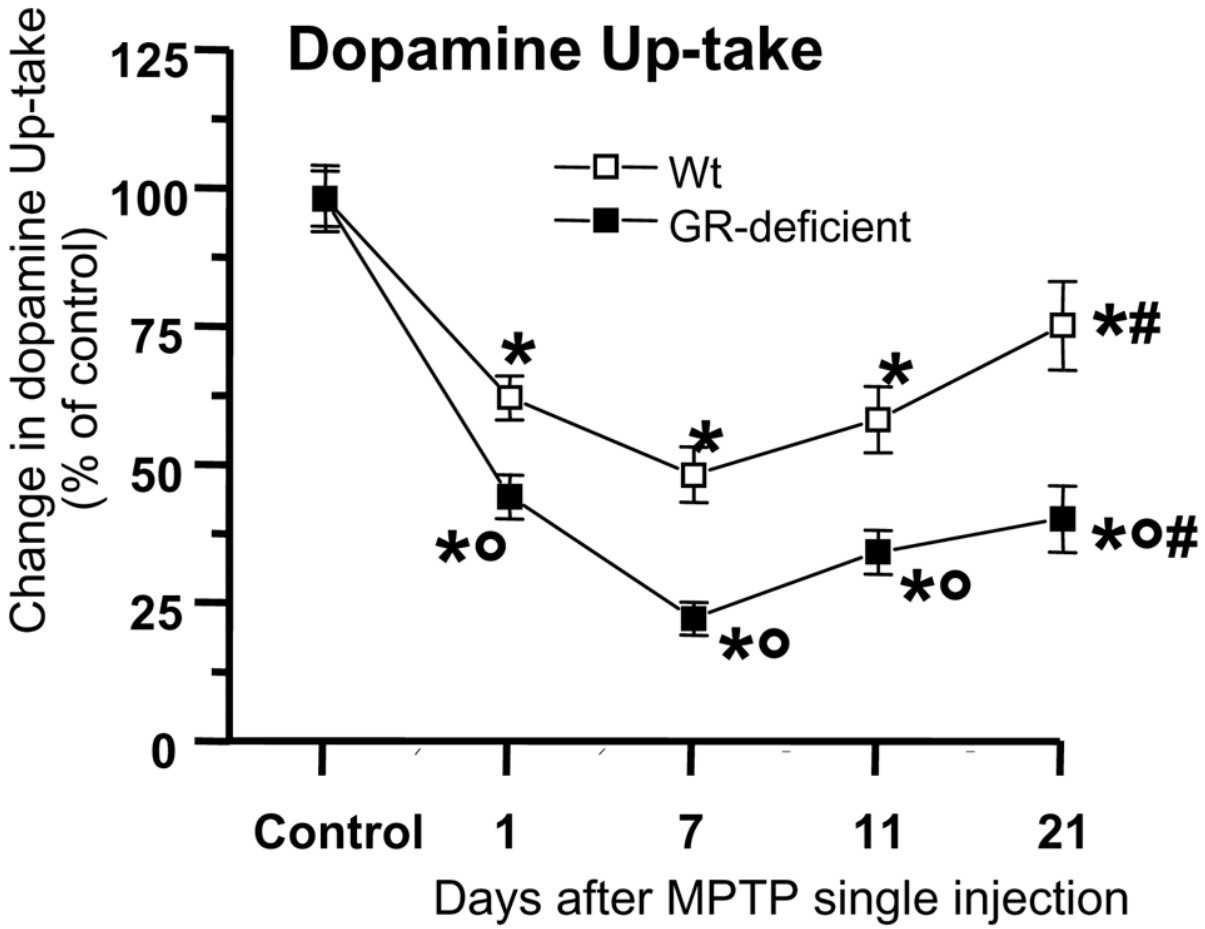

Figure 3. [^{3}H]Dopamine up-take by striatal synaptosomes of Wt and GR-deficient mice at different days after a single MPTP dose. MPTP 55 mg/kg was given intraperitoneally. Mice were killed at the indicated days after MPTP injection. Specific high-affinity neuronal [^{3}H]dopamine up-take was calculated as fentomoles of [^{3}H]dopamine up-take per microgram of protein minus the fentomoles of mazindol up-take. Values are given as percentage changes of controls (mean ± SE, for n = 5–6 mice/group). *P < 0.01 vs. controls, $^{\#}P$ < 0.05 vs. Day 7, and °P < 0.01 vs. Wt (ANOVA followed by Student-Neuman-Keuls post-hoc comparison).

Downloaded from www.fasebj.org to IP 151.97.98.252. *The FASEB Journal* Vol., No. , pp:, November, 2016

Fig. 4

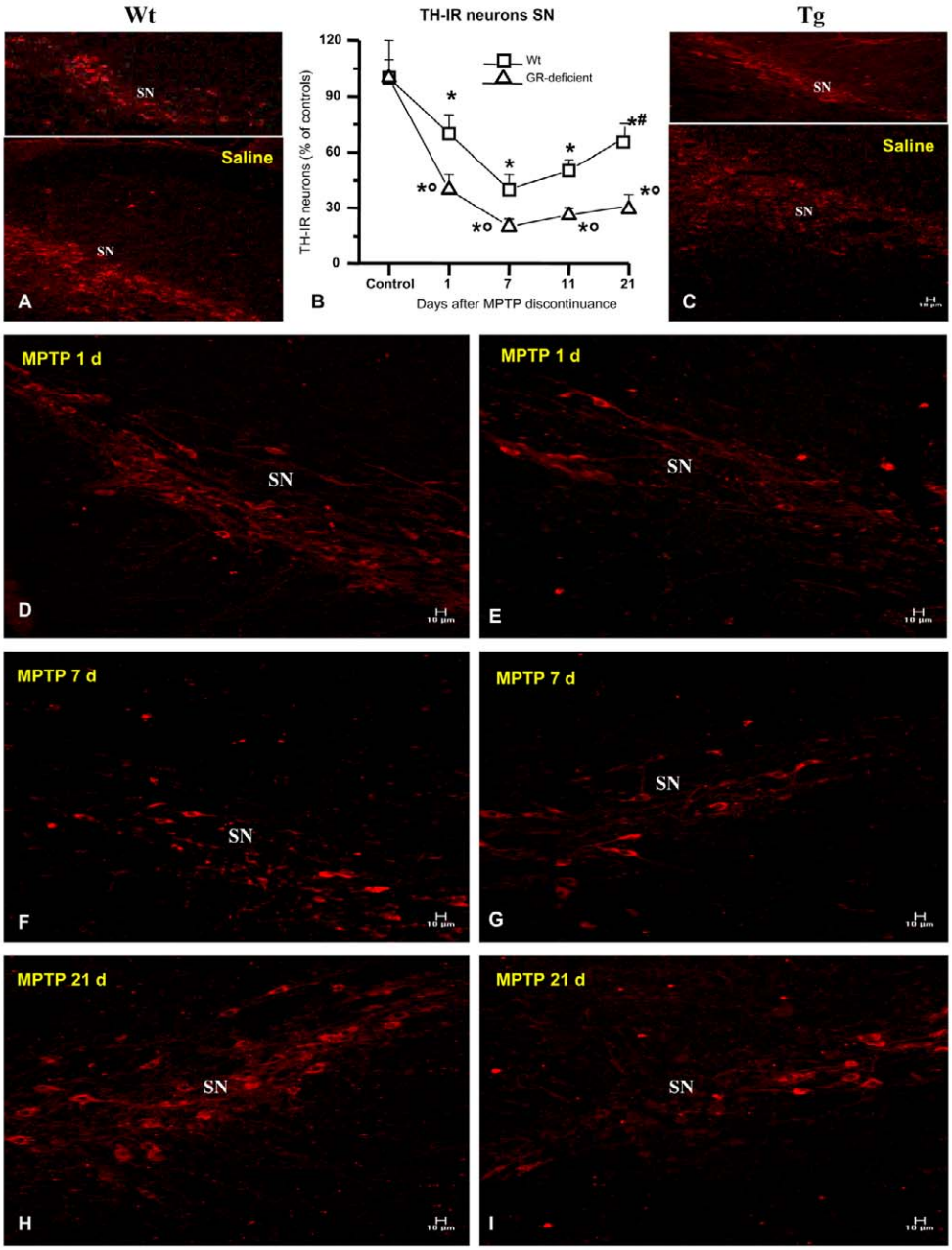

Figure 4. TH immunocytochemistry in the SN of Wt and Tg mice exposed to MPTP. Groups of five Wt or Tg mice per time period received intraperitoneal injections of MPTP HCl 30 mg/kg/day, at 24 h intervals, on 5 consecutive days. Controls were given saline (2.0 ml/kg). On the indicated days after MPTP discontinuance, mice were anesthetized and rapidly perfused transcardially, the brains were carefully removed and processed for immunocytochemistry. TH-immunoreactivity was detected by using either immunoperoxidase (for cell counting; ***B***) or immunofluorescence (***A***, ***C–I***) histochemistry (see Exerimental Procedures section). ***B***) Quantitative values of TH-IR neurons in nigral sections of Wt and Tg mice are expressed as percent of controls (saline-injected mice) and given as mean ± SE (4–5 mice/experimental group; ***B***). Note the earlier and greater TH-IR neuron reduction in Tg compared with Wt mice, at all time tested. **P* < 0.01 vs. controls; #*P* < 0.01 vs. Day 7; °*P* < 0.01 vs. Wt mice (ANOVA followed by Student-Neuman-Keuls post-hoc comparison). ***A***, ***C***) Confocal laser scanning microscopy of TH-IR cell bodies (revealed by CY3, in red) in SN showing no difference in TH immunofluorescent reactions between saline-injected Wt (***A***) or Tg (***C***) mice SN. ***D–E***) One day after MPTP discontinuance, TH-IR cell bodies are dramatically reduced in the SN of Tg (***E***) compared with Wt mice (***D***). ***F–G***) Seven days after MPTP discontinuance, TH-IR neurons are markedly decreased in both Wt (***F***) and Tg (***G***) mice, although a more severe reduction of TH-IR neurons is apparent in Tg mice (***B***). ***H–I***) Twenty-one days after MPTP discontinuance, no trends towards a recovery is observed in Tg (***I***) compared with Wt mice (***H***). 40×. Scale bar 10 μm.

Downloaded from www.fasebj.org to IP 151.97.98.252. *The FASEB Journal* Vol., No. , pp:, November, 2016

Fig. 5

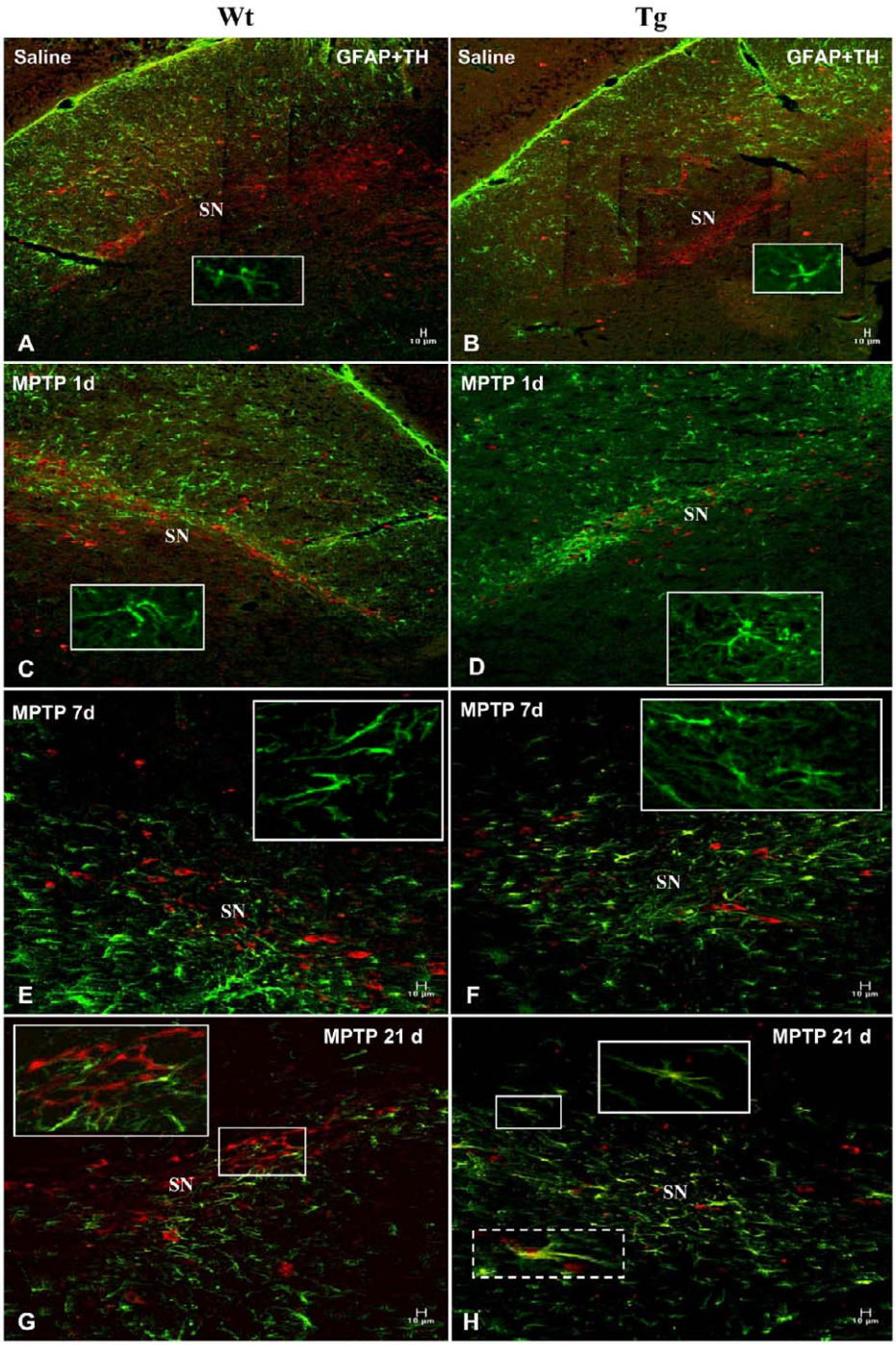

Figure 5. Dual immunocytochemistry of TH and GFAP in the SN of GR-deficient and Wt mice 1–21 days after MPTP discontinuance. Mice were killed at the indicated time after MPTP discontinuance, and mid-brain sections were processed for dual TH and GFAP immunocytochemistry. ***A–B***) Confocal images of GFAP-IR (revealed by FITC, in green) and TH-IR (revealed by CY3, in red) cells showing no difference between Wt (***A***) and Tg (***B***) mice after saline injection. ***C–D***) One day after MPTP discontinuation, GFAP-IR cell invasion of SN is greater in Tg (***D***) compared with Wt mice (***C***). Note the greater astrocyte hypertrophy of Tg (***D***, insert) compared with Wt (***C***, insert) mice; 10×. Scale bar: 10 μm. At 7 days, note the greater hypertrophy of astrocytes and reduced TH-IR cell bodies in Tg (***F***) compared with Wt (***E***) mice. By 21 days, hypertrophic astrocytes were reduced but still present in SN of Wt (***C***, insert). Note an initial recovery of TH-IR cell bodies in SN of Wt mice, in close contact with astrocytic meshworks (***G***, insert). In Tg mice, hypertrophic astrocytes were still present, but only few TH-IR neurons could be localized (***H***). In the insert, an astrocyte appears to engulf a TH-IR cell body (***H***, inserts); 20×. Scale bar: 10 μm.

Downloaded from www.fasebj.org to IP 151.97.98.252. *The FASEB Journal* Vol., No. , pp:, November, 2016

Fig. 6

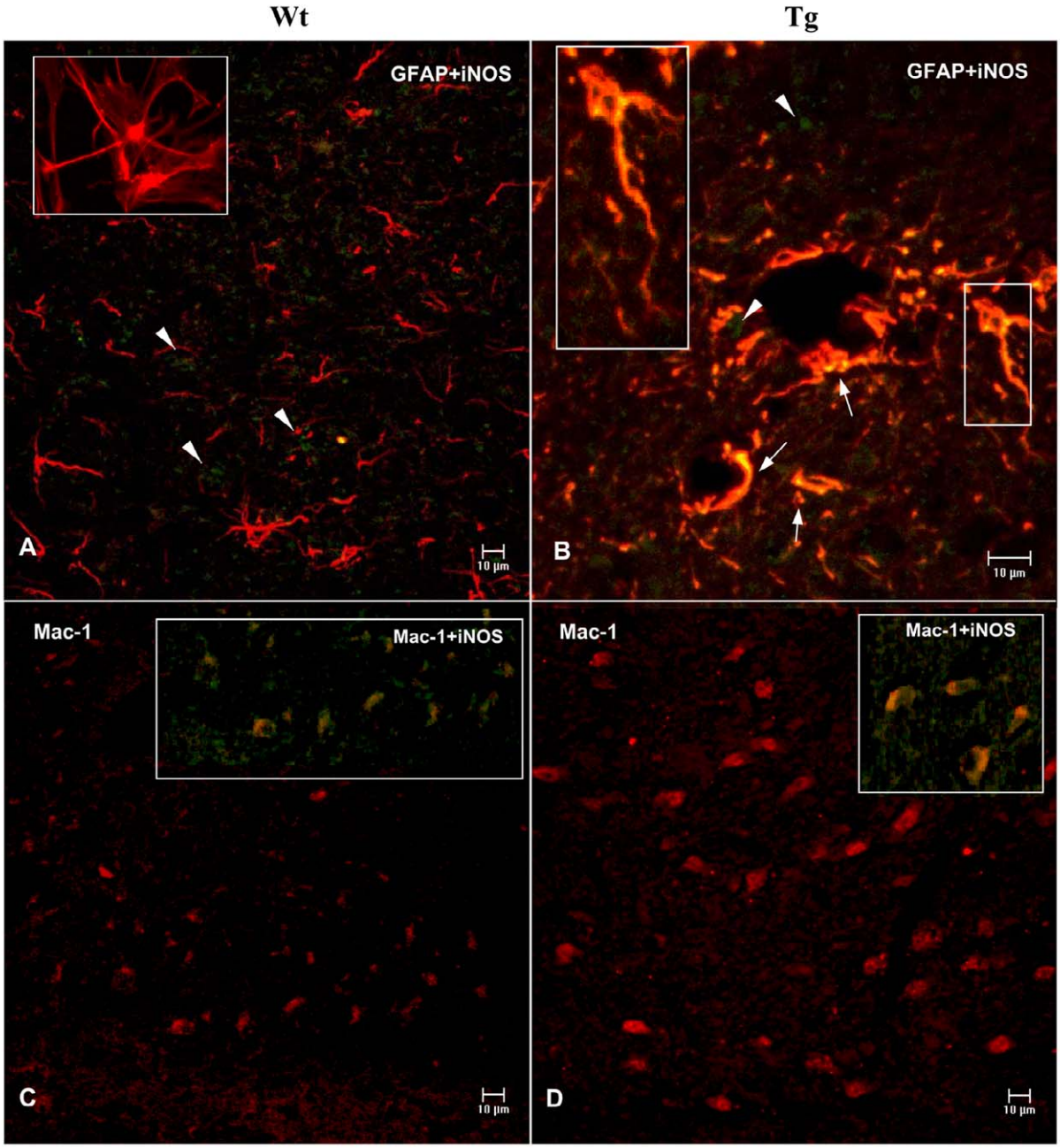

Figure 6. Inducible nitric oxide synthase (iNOS) in activated astrocytes and macrophages/microglia in the SN of GR-deficient and Wt mice 1 day after MPTP exposure. One day after MPTP, nigral sections were processed for dual GFAP and iNOS, or Mac-1 and iNOS immunocytochemistry. ***A–B***) Confocal images of GFAP(revealed by CY3, in red) and iNOS (revealed by FITC, in green) immunofluorescent reactions in Wt (***A***) and Tg (***B***) mice. Note that GFAP-positive and GFAP-negative cells are faintly stained by iNOS in the SN of Wt (***A***, arrowhead) at this time-point. In Tg mice, a strong iNOS immunofluorescent signal was localized in both GFAP-positive (***B***, arrows, insert) and GFAP-negative round- to oval- (***B***, arrowheads) shaped cells, identified as ameboid microglia. Fusion confocal microscopic images reveal complete overlap of GFAP and iNOS in Tg, as revealed by the bright yellow immunofluorescence throughout the cell bodies, nuclei, and processes of nigral Tg astrocytes (***B***, arrow, insert). ***C–D***) Numerous round-shaped Mac-1-IR (revealed by CY3, in red) microglial cells are localized in the SN of GR-deficient (***D***) compared with Wt mice (***A***) on day 1 after MPTP discontinuance. Fusion confocal microscopic images reveal extensive overlap of Mac-1-IR and iNOS, appearing in yellow in Tg (***D***, insert) compared with Wt (***C***, insert) SN.

Downloaded from www.fasebj.org to IP 151.97.98.252. *The FASEB Journal* Vol., No. , pp:, November, 2016

Fig. 7

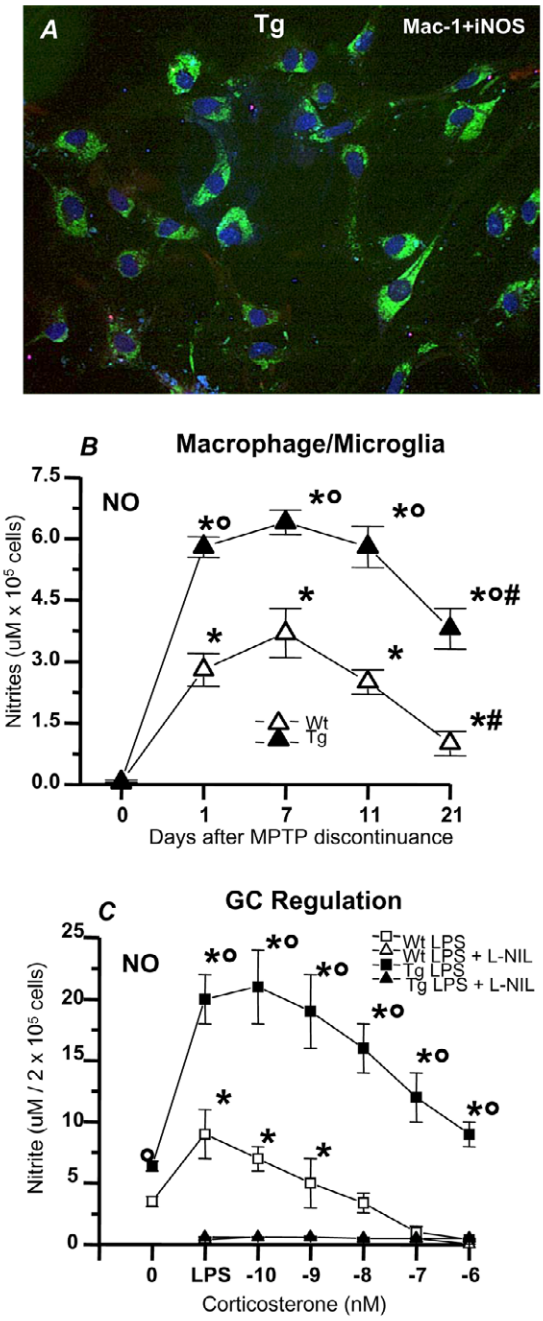

Figure 7. Up-regulation of nitrite production by brain macrophage/microglia of Tg mice following MPTP exposure and lack of inhibition by corticosterone. Groups of six Wt or Tg mice per time period received intraperitoneal injections of MPTP HCl 30 mg/kg/day, at 24 h intervals, on 5 consecutive days. Controls were given saline (2.0 ml/kg). Mice were killed on the indicated days after MPTP discontinuance. At each time-point, the brains (6/group) were dissected, and the isolated adherent cells were cultured for 48 h; nitrite production was determined in cell-free supernatant. ***A)*** Dual immunofluorescence labeling of numerous round-shaped Mac-1-IR (revealed by FITC, in green) microglial cells expressing iNOS (revealed by AMCA, in blue) in GR-deficient cultures on day 1 after MPTP discontinuance. ***B)*** Time-course of nitrite production during MPTP treatment $*P < 0.01$ vs. pertinent controls; $°P < 0.01$ vs. cultures from brains of Wt mice. ***C)*** Regulation of microglial/macrophage-derived NO production by corticosterone on Day 7 after MPTP discontinuance. Nitrite levels were measured before (Time 0) and 24 h after application of LPS (100 ng/ml) with or without the specific iNOS inhibitor L-NIL (20 μM). $*P < 0.01$ vs. Time 0 levels; $°P < 0.01$ vs. cultures from brains of Wt mice at the corresponding time-periods (ANOVA followed by Student-Neuman-Keuls post-hoc comparison).

Downloaded from www.fasebj.org to IP 151.97.98.252. *The FASEB Journal* Vol., No. , pp:, November, 2016

Fig. 8

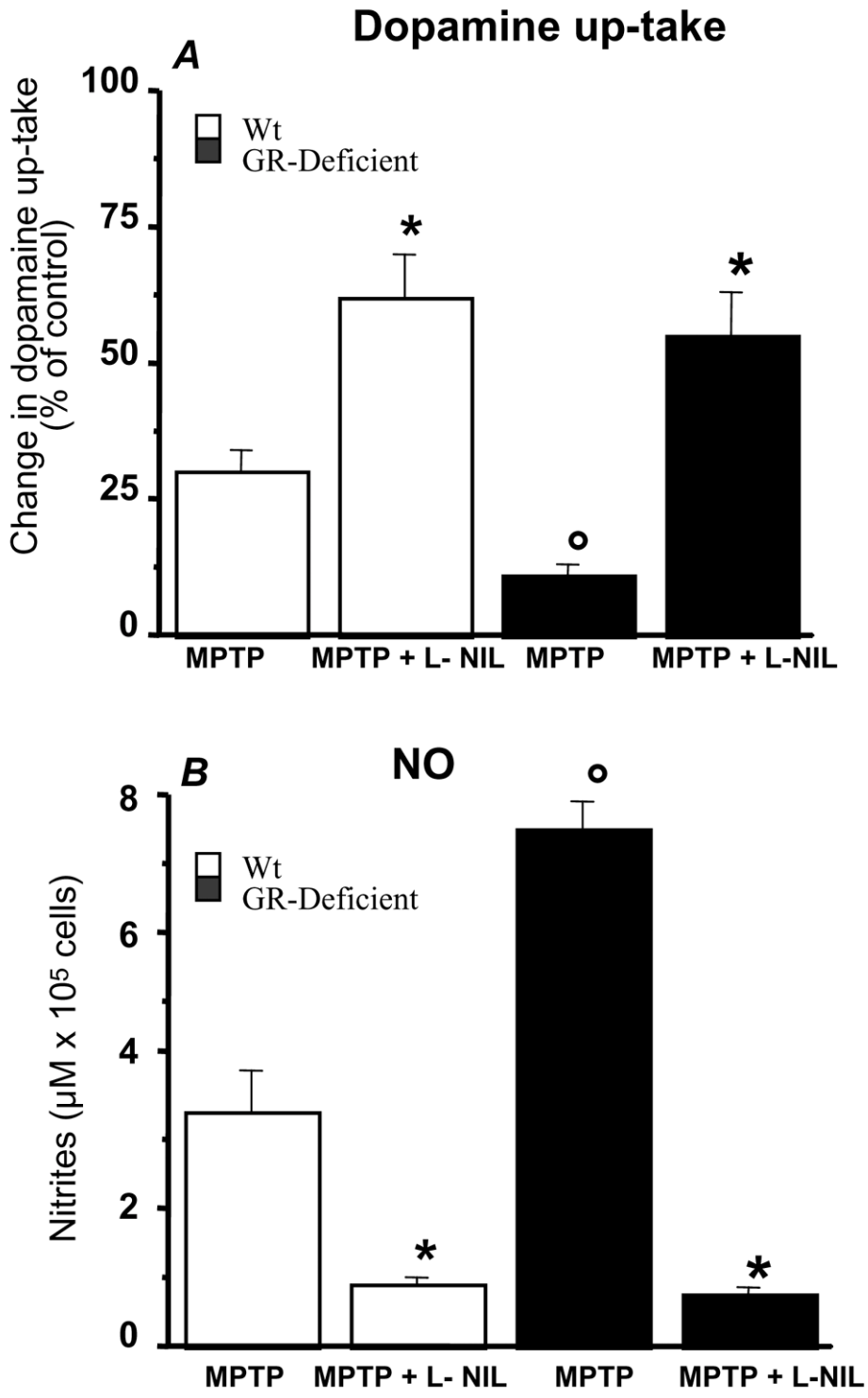

Figure 8. Effect of iNOS inhibition on striatal [^{3}H]Dopamine up-take and macrophage/microglia nitrite production in Wt and GR-deficient mice following MPTP exposure. Wt and GR-deficient mice received or not L-NIL orally (100 µg/ml in the drinking water) starting one day prior to MPTP treatment, according to the established schedule. Mice were killed 7 days after MPTP discontinuation. ***A)*** [^{3}H]dopamine up-take in striatum. Values are presented as the changes in dopamine up-take (expressed as percent of controls ± SE) for *n* = 5–6 mice/group. ***B)*** Nitrite production by macrophage/microglia cultures 7 days after MPTP discontinuance in Wt and GR-deficient mice receiving or not L-NIL treatment. **P* < 0.01 vs. MPTP, within each experimental group; °*P* < 0.01 vs. Wt (ANOVA followed by Student-Neuman-Keuls post hoc comparison).

Downloaded from www.fasebj.org to IP 151.97.98.252. *The FASEB Journal* Vol., No. , pp:, November, 2016

Fig. 9

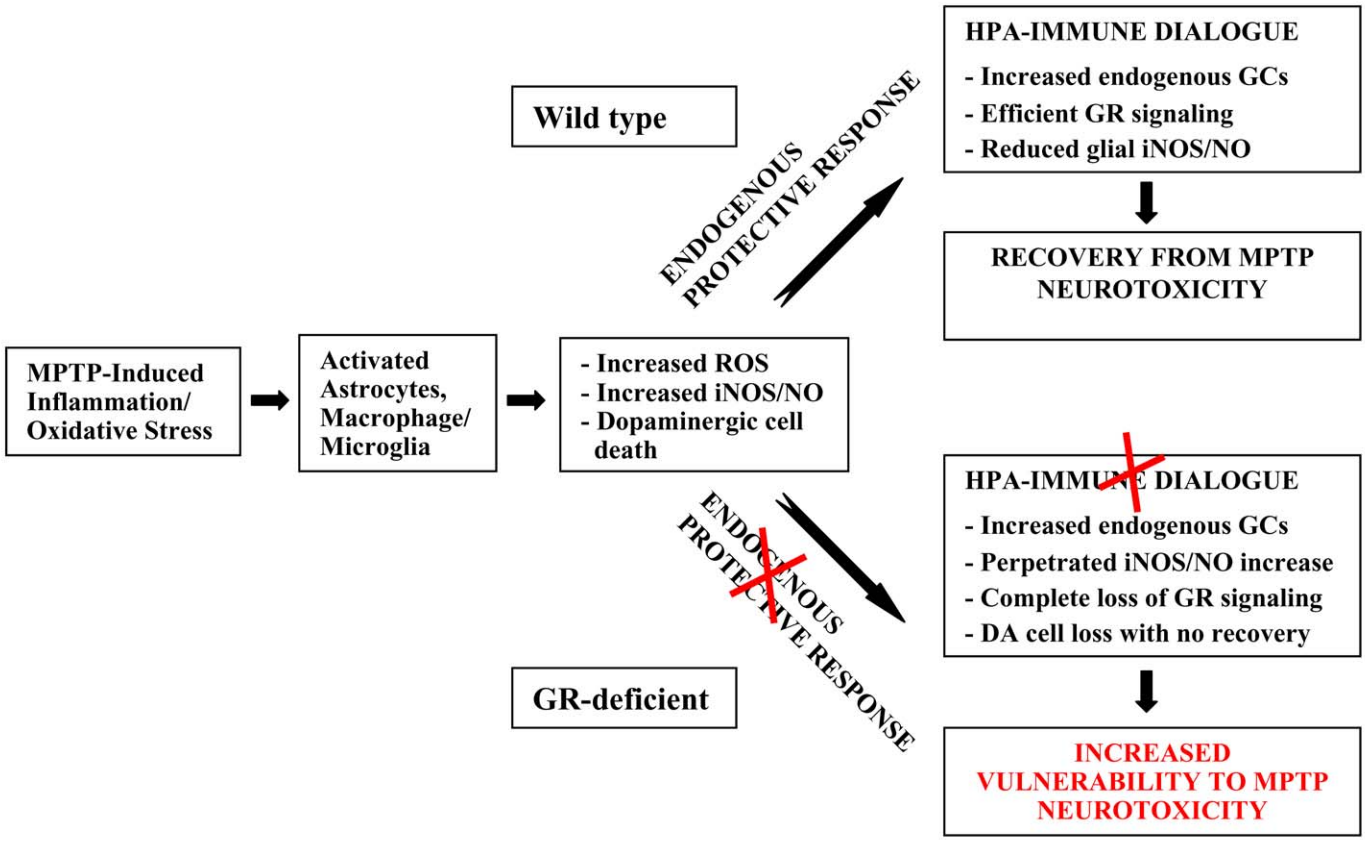

Figure 9. Schematic diagram depicting alteration of GR-NO crosstalk responsible for increased vulnerability to MPTP neurotoxicity. In this model, vulnerability to MPTP-induced impairment of dopaminergic neuron functioning is determined by astroglia response to inflammation and oxidative stress. Efficiency of the HPA-immune dialogue via GR-NO crosstalk represents a critical step for the induction of an "endogenous protective" response. Thus, in Wt mice, efficient GR signaling may reduce glial reactivity leading to reactive oxygen (ROS) and nitrogen species generation, thereby attenuating neuronal loss and stimulating the recovery process. In Tg mice, MPTP induces an earlier and sharper increase in oxidative/nitrosative status, which further impairs GR signaling and exacerbates the GR deficiency at critical times of MPTP-induced dopaminergic neuron degeneration, resulting in dopaminergic neuron demise and failure to recover.

Downloaded from www.fasebj.org to IP 151.97.98.252. *The FASEB Journal* Vol., No. , pp:, November, 2016

THE FASEB JOURNAL
The Journal of the Federation of American Societies for Experimental Biology

Glucocorticoid receptor deficiency increases vulnerability of the nigrostriatal dopaminergic system: critical role of glial nitric oxide

Maria Concetta Morale, Pier Andrea Serra, Maria Rosaria Delogu, et al.

FASEB J published online November 20, 2003
Access the most recent version at doi:10.1096/fj.03-0501fje

Subscriptions Information about subscribing to *The FASEB Journal* is online at http://www.faseb.org/The-FASEB-Journal/Librarian-s-Resources.aspx

Permissions Submit copyright permission requests at: http://www.fasebj.org/site/misc/copyright.xhtml

Email Alerts Receive free email alerts when new an article cites this article - sign up at http://www.fasebj.org/cgi/alerts

α-GalCer now available
C8, C16 & C24:1 Galactosyl(α) Ceramide
Avanti® Polar Lipids, Inc.

Downloaded from www.fasebj.org to IP 151.97.98.252. *The FASEB Journal* Vol., No. , pp:, November, 2016